REPORT No. 521

AN ANALYSIS OF LONGITUDINAL STABILITY IN POWER-OFF FLIGHT WITH CHARTS FOR USE IN DESIGN

By CHARLES H. ZIMMERMAN

SUMMARY

This report presents a discussion of longitudinal stability in gliding flight together with a series of charts with which the stability characteristics of any airplane may be readily estimated.

The first portion of this report is intended, primarily, for students of the subject. The relationships governing stability characteristics are derived from equations of equilibrium referred to moving axes that are tangent and perpendicular to the instantaneous flight path. It is shown that instability of the motion can arise only through an increase of linear and angular momentum in the system during one complete cycle. The interaction of events leading to increase or decrease of momentum during a cycle is explained in detail. The construction of charts showing the effects of the nondimensional parameters C_L, C_D, $\frac{dC_L}{d\alpha}$, $\frac{dC_D}{d\alpha}$, $-m_q$, *and* $-\mu m_\alpha$ *upon the stability characteristics is explained and the effects of the more important of the aerodynamic and mass characteristics of the airplane, as revealed by the charts, are discussed.*

The latter portion of the paper is devoted to a series of 40 related charts with which the dynamic stability of any airplane in power-off flight may be readily estimated. The use of the charts is explained in detail so that reference to the earlier discussion is unnecessary.

INTRODUCTION

The longitudinal stability of aircraft has received very extensive and exhaustive treatment by able writers (see references and bibliography), but the classical treatment of the subject has been rather difficult for those not familiar with higher mathematics. The study reported herein was undertaken with the purpose of making more understandable the mathematical treatment and of preparing a method of estimating stability characteristics that would be sufficiently accurate and rapid to appeal to practical designers.

The section preceding the group of charts for determining stability characteristics in power-off flight is devoted to a derivation, in relatively simple terms, of the mathematical relationships and to a discussion of the formulas. The portion following the group of charts consists of an explanation of the method of using them. It is not necessary to read the first portion in order to use the charts with satisfactory results. All symbols not given in the report cover are defined where used and are also listed in the appendix.

I. ANALYSIS AND DISCUSSION

DERIVATION OF MATHEMATICAL FORMULAS

Definition of stability characteristics.—The stability characteristics of an airplane are those qualities which define the nature of the motion after a deviation from an initial condition of equilibrium. The motion may be periodic, consisting of a series of oscillations having a certain period and rate of increase or decrease in amplitude, or aperiodic with a certain rate of return toward or deviation from the equilibrium position. In many stable airplanes the return to a condition of nonoscillating equilibrium is spoken of as aperiodic or "dead beat" when it is essentially oscillatory in character but very heavily damped.

Fundamental concepts and assumptions.—The forces and moments determining the motion of the airplane are of two kinds: (1) Aerodynamic forces and moments created by movement of the lifting and control surfaces relative to the surrounding air; (2) mass forces and moments arising from the weight and acceleration, angular as well as linear, of the airplane. The fundamental basis of the discussion presented in this report is that at all times there exists a state of equilibrium between the mass forces and moments and the aerodynamic forces and moments.

A complete treatment of the stability of airplanes would be extremely lengthy and very complex. Certain assumptions have therefore been made. As the motion of an airplane is three dimensional, it is to be expected that any treatment of the subject will be incomplete if it neglects certain of the components of the motion. Fortunately, conventional airplanes are symmetrical (within limits here applicable) with respect to the plane that includes the fuselage axis and is perpendicular to the span axis. It is obvious that a longitudinal motion having no component of linear velocity perpendicular to that plane or no component of angular velocity about any axis lying in that plane cannot introduce asymmetric forces or moments. Such motion can therefore be treated as an independent phenomenon.

The longitudinal-stability characteristics will necessarily be affected by any deflection of the lifting or control surfaces. The influence of wing elasticity and of free longitudinal control will not be considered in

the primary analysis because such a consideration would complicate the relationships and obscure the fundamental principles.

It is assumed that forces and moments acting upon the wing and the horizontal tail surfaces vary as the square of the air speed and the first power of the angle of attack of the individual surfaces and that they are not affected by the rate of change of either the air speed or the angle of attack. Also the forces upon the lifting surfaces are assumed not to be affected by the rate of rotation of those surfaces (reference 1).

Each of the foregoing assumptions necessarily involves a certain degree of approximation but they are confirmed by comparison between measured and calculated values of stability characteristics (reference 2 and unpublished data) and are justified by the simplification of the relationships they permit.

Equations of equilibrium.—As has been previously stated, the course of the airplane in flight is determined by the conditions necessary to maintain equilibrium between mass and aerodynamic forces and moments at all times. In steady flight the equilibrium may be expressed by the equations (see fig. 1):

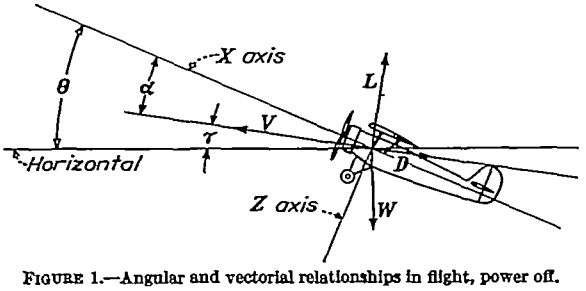

FIGURE 1.—Angular and vectorial relationships in flight, power off.

$$\left.\begin{aligned} W\sin\gamma+\tfrac{1}{2}\rho V^2SC_D&=0 \quad \text{a}\\ W\cos\gamma-\tfrac{1}{2}\rho V^2SC_L&=0 \quad \text{b}\\ \tfrac{1}{2}\rho V^2ScC_m&=0 \quad \text{c}\end{aligned}\right\}(1)$$

where (1a) refers to forces tangent to the instantaneous flight path, (1b) to forces perpendicular to the instantaneous flight path in the plane of symmetry, and (1c) to moments about an axis through the center of gravity and perpendicular to the plane of symmetry. After displacement from the steady-flight condition the equations of equilibrium read:

$$\left.\begin{aligned} W\sin(\gamma+\Delta\gamma)+\tfrac{1}{2}\rho(V+\Delta V)^2S(C_D+\Delta C_D)&=-m\frac{dV}{dt} \quad \text{a}\\ W\cos(\gamma+\Delta\gamma)-\tfrac{1}{2}\rho(V+\Delta V)^2S(C_L+\Delta C_L)&=-mV\frac{d\gamma}{dt} \quad \text{b}\\ \tfrac{1}{2}\rho(V+\Delta V)^2Sc(C_m+\Delta C_m)&=mk_Y{}^2\frac{d^2\theta}{dt^2} \quad \text{c}\end{aligned}\right\}(2)$$

where

$\frac{dV}{dt}$, acceleration tangent to flight path.

$V\frac{d\gamma}{dt}$, centrifugal acceleration normal to the flight path.

$\frac{d^2\theta}{dt^2}$, angular acceleration of airplane about the lateral axis.

Since the effects of angular velocity and of acceleration upon the forces are neglected, ΔC_D may be written as $\Delta\alpha\frac{dC_D}{d\alpha}$ and ΔC_L as $\Delta\alpha\frac{dC_L}{d\alpha}$; ΔC_m may be written as $\Delta\alpha\frac{dC_m}{d\alpha}+\Delta q\frac{dC_m}{dq}$ where $\Delta q=q$, the angular velocity in pitch, since q is zero in the original condition; and ΔV, $\Delta\gamma$, $\Delta\alpha$, and q are small quantities by assumption. Terms involving products of two or more small quantities will be neglected.

Also

$$\begin{aligned}\sin(\gamma+\Delta\gamma)&=\sin\gamma\cos\Delta\gamma+\cos\gamma\sin\Delta\gamma\\ &=\sin\gamma+\Delta\gamma\cos\gamma\end{aligned}$$

and

$$\begin{aligned}\cos(\gamma+\Delta\gamma)&=\cos\gamma\cos\Delta\gamma-\sin\gamma\sin\Delta\gamma\\ &=\cos\gamma-\Delta\gamma\sin\gamma\end{aligned}$$

Then:

$$\left.\begin{aligned} W\sin\gamma+W\Delta\gamma\cos\gamma+\tfrac{1}{2}\rho V^2SC_D+\rho VSC_D\Delta V+\tfrac{1}{2}\rho V^2S\frac{dC_D}{d\alpha}\Delta\alpha&=-m\frac{dV}{dt} \quad \text{a}\\ W\cos\gamma-W\Delta\gamma\sin\gamma-\tfrac{1}{2}\rho V^2SC_L-\rho VSC_L\Delta V-\tfrac{1}{2}\rho V^2S\frac{dC_L}{d\alpha}\Delta\alpha&=-mV\frac{d\gamma}{dt} \quad \text{b}\\ \tfrac{1}{2}\rho V^2ScC_m+\rho VScC_m\Delta V+\tfrac{1}{2}\rho V^2Sc\frac{dC_m}{d\alpha}\Delta\alpha+\tfrac{1}{2}\rho V^2Sc\frac{dC_m}{dq}q&=mk_Y{}^2\frac{d^2\theta}{dt^2} \quad \text{c}\end{aligned}\right\}(3)$$

Subtracting (1) from (3)

$$\left.\begin{aligned} W\Delta\gamma\cos\gamma+\rho VSC_D\Delta V+\tfrac{1}{2}\rho V^2S\frac{dC_D}{d\alpha}\Delta\alpha&=-m\frac{dV}{dt} \quad \text{a}\\ -W\Delta\gamma\sin\gamma-\rho VSC_L\Delta V-\tfrac{1}{2}\rho V^2S\frac{dC_L}{d\alpha}\Delta\alpha&=-mV\frac{d\gamma}{dt} \quad \text{b}\\ \rho VScC_m\Delta V+\tfrac{1}{2}\rho V^2Sc\frac{dC_m}{dq}q+\tfrac{1}{2}\rho V^2Sc\frac{dC_m}{d\alpha}\Delta\alpha&=mk_Y{}^2\frac{d^2\theta}{dt^2} \quad \text{c}\end{aligned}\right\}(4)$$

From equations (1)

$$W\cos\gamma=\frac{1}{2}\rho V^2SC_L$$

$$W\sin\gamma=-\frac{1}{2}\rho V^2SC_D$$

$$C_m=0$$

Therefore,

$$\left.\begin{aligned}
&-\frac{1}{2}\rho V^2SC_L\Delta\gamma-\rho VSC_D\Delta V-\frac{1}{2}\rho V^2S\frac{dC_D}{d\alpha}\Delta\alpha=m\frac{dV}{dt} && \text{a}\\
&\frac{1}{2}\rho V^2SC_D\Delta\gamma-\rho VSC_L\Delta V-\frac{1}{2}\rho V^2S\frac{dC_L}{d\alpha}\Delta\alpha=-mV\frac{d\gamma}{dt} && \text{b}\\
&\frac{1}{2}\rho V^2Sc\frac{dC_m}{dq}q+\frac{1}{2}\rho V^2Sc\frac{dC_m}{d\alpha}\Delta\alpha=mk_Y^2\frac{d^2\theta}{dt^2} && \text{c}
\end{aligned}\right\}(5)$$

Dividing (5a) and (5b) by $\frac{1}{2}\rho V^2S$ and (5c) by ρSV

$$\left.\begin{aligned}
&-C_L\Delta\gamma-2C_D\frac{\Delta V}{V}-\frac{dC_D}{d\alpha}\Delta\alpha=2\frac{m}{\rho SV}\frac{\frac{dV}{dt}}{V} && \text{a}\\
&C_D\Delta\gamma-2C_L\frac{\Delta V}{V}-\frac{dC_L}{d\alpha}\Delta\alpha=-2\frac{m}{\rho SV}\frac{d\gamma}{dt} && \text{b}\\
&\frac{1}{2}Vc\frac{dC_m}{dq}q+\frac{1}{2}Vc\frac{dC_m}{d\alpha}\Delta\alpha=\frac{mk_Y^2}{\rho SV}\frac{d^2\theta}{dt^2} && \text{c}
\end{aligned}\right\}(6)$$

Let

$\frac{m}{\rho SV}=\tau$ (after Glauert, reference 3)

$\frac{\Delta V}{V}=\Delta V'$

$\frac{\frac{dV}{dt}}{V}=\frac{dV'}{dt}$

$$\left.\begin{aligned}
&-C_L\Delta\gamma-2C_D\Delta V'-\frac{dC_D}{d\alpha}\Delta\alpha=2\tau\frac{dV'}{dt} && \text{a}\\
&C_D\Delta\gamma-2C_L\Delta V'-\frac{dC_L}{d\alpha}\Delta\alpha=-2\tau\frac{d\gamma}{dt} && \text{b}\\
&\frac{1}{2}Vc\frac{dC_m}{dq}q+\frac{1}{2}Vc\frac{dC_m}{d\alpha}\Delta\alpha=\tau k_Y^2\frac{d^2\theta}{dt^2} && \text{c}
\end{aligned}\right\}(7)$$

Equations (7a) and (7b) are nondimensional and the only variables are $\Delta\gamma$, $\Delta V'$, and $\Delta\alpha$. In order to reduce (7c) to a comparable form it is necessary to rewrite $\frac{dC_m}{dq}$, which is the only constant in the equations not in readily usable form, and to express θ in terms of γ and α.

The greater portion of the change in pitching moment produced by rotation occurs because the rotation changes the angle of attack of the tail surfaces. A positive rotation q causes the tail to move downward with a velocity, relative to the center of gravity, equal to ql where l is the distance from the center of gravity to the mean quarter-chord point of the horizontal surfaces. The tangent of the change in angle of attack at the tail is $\tan\Delta\alpha_t=ql/V$ which may be replaced by $\Delta\alpha_t=ql/V$ for the small angles under consideration. The change in moment due to the change in the angle of attack at the tail is

$$\Delta M_t=\frac{1}{2}\rho V^2lS_t\eta_t\frac{dC_{Z_t}}{d\alpha_t}\Delta\alpha_t$$

where $\frac{dC_{Z_t}}{d\alpha_t}$, slope of normal-force curve of tail surfaces.

S_t, area of horizontal tail surfaces.

η_t, tail efficiency.

or, in coefficient form,

$$\Delta C_{m_t}=\frac{l}{c}\frac{S_t}{S}\eta_t\frac{dC_{Z_t}}{d\alpha_t}\frac{ql}{V}$$

Introducing an empirical factor K to allow for wing damping

$$\frac{dC_m}{dq}=K\frac{l}{c}\frac{S_t}{S}\eta_t\frac{dC_{Z_t}}{d\alpha_t}\frac{l}{V}$$

Therefore (7c) may be rewritten as

$$\frac{1}{2}l^2K\frac{dC_{Z_t}}{d\alpha_t}\frac{S_t}{S}\eta_tq+\frac{1}{2}Vc\frac{dC_m}{d\alpha}\Delta\alpha=\tau k_Y^2\frac{d^2\theta}{dt^2} \qquad (8)$$

Dividing (8) through by k_Y^2 and multiplying by τ to make the expression nondimensional,

$$\tau\frac{1}{2}\frac{l^2}{k_Y^2}K\frac{dC_{Z_t}}{d\alpha_t}\frac{S_t}{S}\eta_tq+\frac{1}{2}\frac{mc}{\rho Sk_Y^2}\frac{dC_m}{d\alpha}\Delta\alpha=\tau^2\frac{d^2\theta}{dt^2} \qquad (9)$$

Letting $\frac{m}{\rho Sl}=\mu$ (reference 3)

$$\frac{1}{2}\frac{l^2}{k_Y^2}K\frac{dC_{Z_t}}{d\alpha_t}\frac{S_t}{S}\tau\eta_tq+\frac{1}{2}\mu\frac{lc}{k_Y^2}\frac{dC_m}{d\alpha}\Delta\alpha=\tau^2\frac{d^2\theta}{dt^2} \qquad (10)$$

For convenience let

$$\eta_t\frac{1}{2}\frac{l^2}{k_Y^2}K\frac{dC_{Z_t}}{d\alpha_t}\frac{S_t}{S}=m_q$$

and

$$\frac{1}{2}\frac{lc}{k_Y^2}\frac{dC_m}{d\alpha}=m_\alpha$$

$$m_q\tau q+\mu m_\alpha\Delta\alpha=\tau^2\frac{d^2\theta}{dt^2} \qquad (11)$$

Since $\theta=(\alpha+\gamma)$ and $q=\frac{d\theta}{dt}$ (see fig. 1), q and θ may be replaced by α and γ reducing the number of variables in equations (7a), (7b), and (11) to three. These equations are rewritten as,

$$\left.\begin{aligned}
&-C_L\Delta\gamma-2C_D\Delta V'-\frac{dC_D}{d\alpha}\Delta\alpha=2\tau\frac{dV'}{dt} && \text{a}\\
&C_D\Delta\gamma-2C_L\Delta V'-\frac{dC_L}{d\alpha}\Delta\alpha=-2\tau\frac{d\gamma}{dt} && \text{b}\\
&m_q\tau\left(\frac{d\alpha}{dt}+\frac{d\gamma}{dt}\right)+\mu m_\alpha\Delta\alpha=\tau^2\left(\frac{d^2\alpha}{dt^2}+\frac{d^2\gamma}{dt^2}\right) && \text{c}
\end{aligned}\right\}(12)$$

The foregoing equations of equilibrium must each be satisfied at each instant (neglecting approximations assumed) of flight. It is obvious that each of the variables $\Delta\gamma$, $\Delta\alpha$, and $\Delta V'$ will affect each of the others, and it is reasonable to assume that, if any one of them follows a regular scheme of variation with time, then the others will vary according to the same scheme.

Assume therefore that the variables change according to the exponential expressions:

$$\Delta\gamma = Ae^{\lambda t}$$
$$\Delta\alpha = Be^{\lambda t}$$
$$\Delta V' = Ce^{\lambda t}$$

(In mathematical terms $e^{\lambda t}$ is an integrating factor.) where

A, B, and C are constants depending on the magnitude of the initial disturbance.

e, the base of natural logarithms=2.71828.

λ, an arbitrary constant.

t, time in seconds.

It appears that if λ is positive $\Delta\gamma$, $\Delta\alpha$, and $\Delta V'$ will increase with time and therefore the motion will be unstable. If λ is negative the departures from the condition of steady flight will decrease and the motion will be stable.

Now if

$$\Delta\gamma = Ae^{\lambda t}$$
$$\frac{d\gamma}{dt} = A\lambda e^{\lambda t}$$
$$\frac{d^2\gamma}{dt^2} = A\lambda^2 e^{\lambda t}$$
etc.

Substituting in (12)

$$\left.\begin{aligned} &-C_L Ae^{\lambda t} - 2C_D Ce^{\lambda t} - \frac{dC_D}{d\alpha}Be^{\lambda t} = 2\tau\lambda Ce^{\lambda t} && \text{a}\\ &C_D Ae^{\lambda t} - 2C_L Ce^{\lambda t} - \frac{dC_L}{d\alpha}Be^{\lambda t} = -2\tau A\lambda e^{\lambda t} && \text{b}\\ &m_q\tau(B\lambda e^{\lambda t} + A\lambda e^{\lambda t}) + \mu m_\alpha Be^{\lambda t} = \tau^2(\lambda^2 Be^{\lambda t} + \lambda^2 Ae^{\lambda t}) && \text{c} \end{aligned}\right\} (13)$$

Each of the equations may be divided by $e^{\lambda t}$

$$\left.\begin{aligned} &-C_L A - 2C_D C - \frac{dC_D}{d\alpha}B = 2\tau\lambda C && \text{a}\\ &C_D A - 2C_L C - \frac{dC_L}{d\alpha}B = -2\tau\lambda A && \text{b}\\ &m_q\tau\lambda(A+B) + \mu m_\alpha B = (\tau\lambda)^2(A+B) && \text{c} \end{aligned}\right\} (14)$$

From (14b)

$$C = \frac{2\tau\lambda A + C_D A - \frac{dC_L}{d\alpha}B}{2C_L}$$

Also, since τ and λ do not appear except in the product $\tau\lambda$, let $\lambda' = \tau\lambda$

Substituting in (14a)

$$-C_L A - \frac{C_D}{C_L}\left(2\lambda' A + C_D A - \frac{dC_L}{d\alpha}B\right) - \frac{dC_D}{d\alpha}B = \frac{\lambda'}{C_L}\left(2\lambda' A + C_D A - \frac{dC_L}{d\alpha}B\right)$$

Multiplying by C_L

$$-C_L^2 A - 2C_D\lambda' A - C_D^2 A + C_D\frac{dC_L}{d\alpha}B - C_L\frac{dC_D}{d\alpha}B = 2(\lambda')^2 A + \lambda' C_D A - \lambda'\frac{dC_L}{d\alpha}B$$

or, since $C_L^2 + C_D^2 = C_R^2$

$$A[+C_R^2 + 3C_D\lambda' + 2(\lambda')^2] = B\left(+C_D\frac{dC_L}{d\alpha} - C_L\frac{dC_D}{d\alpha} + \lambda'\frac{dC_L}{d\alpha}\right)$$

Therefore,

$$\frac{A}{B} = \frac{C_D\frac{dC_L}{d\alpha} - C_L\frac{dC_D}{d\alpha} + \lambda'\frac{dC_L}{d\alpha}}{C_R^2 + 3C_D\lambda' + 2(\lambda')^2}$$

Also from (14c)

$$A[m_q\lambda' - (\lambda')^2] = B[(\lambda')^2 - m_q\lambda' - \mu m_\alpha]$$

Therefore,

$$\frac{A}{B} = \frac{\mu m_\alpha + m_q\lambda' - (\lambda')^2}{-m_q\lambda' + (\lambda')^2}$$

It therefore appears that equilibrium at all times is possible when,

$$\frac{C_D\frac{dC_L}{d\alpha} - C_L\frac{dC_D}{d\alpha} + \lambda'\frac{dC_L}{d\alpha}}{C_R^2 + 3C_D\lambda' + 2(\lambda')^2} = \frac{\mu m_\alpha + m_q\lambda' - (\lambda')^2}{-m_q\lambda' + (\lambda')^2} \quad (15)$$

or

$$[-m_q\lambda' + (\lambda')^2]\left(C_D\frac{dC_L}{d\alpha} - C_L\frac{dC_D}{d\alpha} + \lambda'\frac{dC_L}{d\alpha}\right) = [C_R^2 + 3C_D\lambda' + 2(\lambda')^2][\mu m_\alpha + m_q\lambda' - (\lambda')^2]$$

Expansion of this relationship and collection of terms give the biquadratic expression

$$(\lambda')^4 + (\lambda')^3\left[-m_q + \frac{1}{2}\left(3C_D + \frac{dC_L}{d\alpha}\right)\right] + (\lambda')^2\left[-m_q\frac{1}{2}\left(3C_D + \frac{dC_L}{d\alpha}\right) - \mu m_\alpha + \frac{1}{2}\left(C_D\frac{dC_L}{d\alpha} - C_L\frac{dC_D}{d\alpha} + C_R^2\right)\right] + \lambda'\left[-m_q\frac{1}{2}\left(C_D\frac{dC_L}{d\alpha} - C_L\frac{dC_D}{d\alpha} + C_R^2\right) - \frac{3}{2}C_D\mu m_\alpha\right] - \mu m_\alpha\frac{C_R^2}{2} = 0 \quad (16)$$

For simplicity the biquadratic may be expressed as:

$$A(\lambda')^4 + B(\lambda')^3 + C(\lambda')^2 + D\lambda' + E = 0 \quad (17)$$

where

$$A = 1$$
$$B = \left[-m_q + \frac{1}{2}\left(3C_D + \frac{dC_L}{d\alpha}\right)\right]$$
$$C = \left[-m_q\frac{1}{2}\left(3C_D + \frac{dC_L}{d\alpha}\right) - \mu m_\alpha + \frac{1}{2}\left(C_D\frac{dC_L}{d\alpha} - C_L\frac{dC_D}{d\alpha} + C_R^2\right)\right]$$
$$D = \left[-m_q\frac{1}{2}\left(C_D\frac{dC_L}{d\alpha} - C_L\frac{dC_D}{d\alpha} + C_R^2\right) - \frac{3}{2}C_D\mu m_\alpha\right]$$
$$E = -\frac{C_R^2}{2}\mu m_\alpha$$

Unfortunately there is no simple, direct method of solving biquadratics. It is possible, however, to factor a biquadratic into two quadratics, each of which is susceptible to direct solution.

The biquadratic

$$(\lambda')^4+B(\lambda')^3+C(\lambda')^2+D\lambda'+E=0$$

may be replaced by the expression

$$[(\lambda')^2+a_1\lambda'+b_1][(\lambda')^2+a_2\lambda'+b_2]=0$$

from which

$$\left.\begin{aligned}&\text{a}\quad \lambda'=-\frac{a_1}{2}\pm\sqrt{\left(\frac{a_1}{2}\right)^2-b_1}\\ &\text{b}\quad \lambda'=-\frac{a_2}{2}\pm\sqrt{\left(\frac{a_2}{2}\right)^2-b_2}\end{aligned}\right\}(18)$$

or

It appears that

$$\begin{aligned}B&=a_1+a_2\\ C&=a_1a_2+b_1+b_2\\ D&=a_1b_2+a_2b_1\\ E&=b_1b_2\end{aligned}$$

The general case may be worked out as follows:

$$\begin{aligned}a_2&=B-a_1\\ C&=a_1(B-a_1)+b_1+b_2\\ D&=a_1b_2+(B-a_1)b_1\\ b_2&=\frac{E}{b_1}\end{aligned}$$

Therefore,

$$\left.\begin{aligned}&\text{a}\quad C=a_1(B-a_1)+b_1+\frac{E}{b_1}\\ &\text{b}\quad D=a_1\frac{E}{b_1}+(B-a_1)b_1\end{aligned}\right\}(19)$$

Dropping the subscripts:

$$\left.\begin{aligned}&\text{a}\quad a=\frac{B}{2}\pm\sqrt{\left(\frac{B}{2}\right)^2-C+b+\frac{E}{b}}\\ &\text{b}\quad a=\frac{b^2B-bD}{b^2-E}\end{aligned}\right\}(20)$$

and

These relations can be solved by plotting the curves of b against a. There are two intersections of these curves, in general, corresponding respectively to a_1, b_1, and to a_2, b_2.

Also from (19)

$$\left.\begin{aligned}&\text{a}\quad \frac{E}{b}=C-b-a(B-a)\\ &\text{b}\quad D=aC-ab-a^2(B-a)+b(B-a)\\ &\text{c}\quad b=\frac{D-aC+a^2B-a^3}{B-2a}\end{aligned}\right\}(21)$$

Substituting (21c) in (19a)

$$C=a(B-a)+\left(\frac{D-aC+a^2B-a^3}{B-2a}\right)+E\left(\frac{B-2a}{D-aC+a^2B-a^3}\right)\qquad(22)$$

or

$$\begin{aligned}&a^6-a^5(3B)+a^4(3B^2+2C)\\ &-a^3(B^3+4BC)+a^2(2B^2C+BD+C^2-4E)\\ &-a(B^2D+BC^2-4EB)+BCD-D^2-B^2E=0\end{aligned}\qquad(23)$$

By use of the foregoing relationships the coefficients of the quadratics may be determined with as high a degree of accuracy as desired by graphical means or by trial substitutions.

At first glance it appears that a 6th-power equation such as (23) would be harder to solve than a 4th-power equation such as (17). In equation (17), however, the complex roots must be obtained; whereas in (23) it is necessary to solve only for the real values. Equation (23) is useful from a practical standpoint chiefly in obtaining accurate values of a_2 by making trial substitutions from approximate values obtained from the expression for a_2 given on page 6. Because of the very small value of a_2 it is generally not necessary to include the terms in (23) that contain powers of a_2 higher than the third.

Significance of λ'.—As appears in equations (18), there are possible either 4 real values of λ', 2 real and 1 pair of complex values, or 2 pairs of complex values. The values of B, C, and D in the normal flying range of conventional airplanes are always positive because of the signs and magnitudes of their constituent factors. It is obvious that no positive real value of λ' can satisfy the biquadratic unless E is negative but that if E is negative there is such a solution for λ'. A positive real value of λ' signifies an aperiodic divergence. If $-\mu m_\alpha$ is positive corresponding to static stability, then E is positive and the biquadratic expression indicates no possibility of an aperiodic divergence.

The values of B, C, D, and E are, in general, such that the solution for λ' gives two pairs of complex values. It can be shown by mathematical reasoning not essential to this treatment that an expression of $Ke^{\lambda' t'}$—where $\lambda'=\zeta'\pm i\psi'$ and where K, ζ', and ψ' are constants and $i=\sqrt{-1}$ — can be replaced by an equivalent expression, $K'e^{\zeta' t'}\cos(\psi' t'-\delta)$ where K' and δ are new constants. Therefore $\Delta\gamma=A\,e^{\lambda' t'}$ may be replaced by $\Delta\gamma=A'e^{\zeta' t'}\cos(\psi' t'-\delta)$ and similarly for the other variables. It appears that the motion indicated by a complex root is therefore made up of sinusoidal variations of the angle of attack, angle of attitude, angle of the flight path, and velocity along the flight path and that the amplitudes of the oscillations increase or decrease with time depending upon whether ζ' is positive or negative. From equations (18) it appears that

$$\zeta_1'=-\frac{1}{2}a_1$$

$$\zeta_2'=-\frac{1}{2}a_2$$

$$\psi_1'=\sqrt{b_1-\left(\frac{a_1}{2}\right)^2}$$

$$\psi_2'=\sqrt{b_2-\left(\frac{a_2}{2}\right)^2}$$

where ζ_1', ζ_2', ψ_1', and ψ_2' express the stability characteristics of the airplane.

From the expression $\Delta\gamma=A'e^{\zeta' t'}\cos(\psi' t'-\delta)$ the period of the oscillation is $P'=\frac{2\pi}{\psi'}$ and the time for the oscillation to damp to one-half amplitude from any instant chosen as the time of starting is $T'=-\frac{0.693}{\zeta'}$. Since λ' was set equal to $\lambda\tau$ during the derivation, P' and T' are in units of time which are equal to $\tau=\frac{\mu l}{V}$ seconds or the time in seconds necessary for the airplane to travel the length l at the velocity V multiplied by the relative-density factor μ. Therefore the final expression for the time in seconds for the oscillation to decrease to one-half amplitude is

$$T=\frac{-0.693}{\zeta'}\tau=\frac{-0.693}{\zeta'}\frac{m}{\rho SV}$$
$$=\frac{-0.313}{\zeta'}\sqrt{\frac{W}{S}C_L} \qquad (24)$$

under standard conditions; and the period in seconds is

$$P=\frac{2\pi}{\psi'}\tau$$
$$=\frac{2.83}{\psi'}\sqrt{\frac{W}{S}C_L} \qquad (25)$$

under standard conditions.

Substituting for a in equation (23):

$$(2\zeta')^6+(2\zeta')^5(3B)+(2\zeta')^4(3B^2+2C)$$
$$+(2\zeta')^3(B^3+4BC)+(2\zeta')^2(2B^2C+BD+C^2-4E)$$
$$+(2\zeta')(B^2D+BC^2-4EB)+BCD-D^2-B^2E=0 \qquad (26)$$

From equation (21)

$$(\psi')^2=\frac{D+2\zeta' C+3(\zeta')^2B+4(\zeta')^3}{B+4\zeta'} \qquad (27)$$

Reference to equation (26) reveals that from the values of B, C, D, and E in the normal-flying ranges the coefficients of the terms in $2\zeta'$ will all be positive. Therefore a positive real value of ζ' can exist only if $(BCD-D^2-B^2E)$ is negative. This fact was first pointed out by Routh (reference 4) by a somewhat different derivation and the factor is known as "Routh's Discriminant."

There has been developed in reference 1 an approximation for the case when D and E are small with respect to B and C by assuming that

$$a_1=B$$
$$b_1=C$$

Then

$$D=Bb_2+a_2C$$
$$E=Cb_2$$

or

$$b_2=\frac{E}{C}$$

and

$$a_2=\frac{D}{C}-\frac{BE}{C^2}$$

It follows that,

$$\zeta_1'=-\frac{B}{2} \qquad (28)$$

$$\psi_1'=\sqrt{C-\left(\frac{B}{2}\right)^2} \qquad (29)$$

$$\zeta_2'=-\frac{1}{2}\left(\frac{D}{C}-\frac{BE}{C^2}\right) \qquad (30)$$

$$\psi_2'=\sqrt{\frac{E}{C}-\frac{1}{4}\left(\frac{D}{C}-\frac{BE}{C^2}\right)^2} \qquad (31)$$

These approximate expressions are generally used and are satisfactory for most cases encountered.

Since B and C are large in the normal-flight range, values of ζ_1' and ψ_1' define a very heavily damped oscillation which is, in general, of short period. This oscillation is unimportant, except possibly in special cases above the stall; throughout the remainder of the report ζ' and ψ' will be used without the subscripts to refer to the slightly damped phugoid oscillation previously defined by ζ_2' and ψ_2'.

Derivation of expression describing the sinusoidal motion.—The expression $\Delta\gamma=Ae^{\lambda t}=Ae^{\lambda' t'}$ can be

replaced by the equivalent expression $\Delta\gamma=A'e^{t'\prime\prime}\cos(\psi't'-\delta)$ where A' and δ depend upon the instant from whence time is taken as zero. If time is zero when $\Delta\gamma$ is at a point of maximum amplitude $A'=\Delta\gamma_0$ and $\delta=0$ so that

$$\Delta\gamma=\Delta\gamma_0 e^{t'\prime\prime}\cos\psi't' \tag{32}$$

It follows that

$$\Delta\alpha=\Delta\alpha_0 e^{t'\prime\prime}\cos(\psi't'-\delta_1) \tag{33}$$

$$\Delta V'=\Delta V_0' e^{t'\prime\prime}\cos(\psi't'-\delta_2) \tag{34}$$

$$\Delta\theta=\Delta\theta_0 e^{t'\prime\prime}\cos(\psi't'-\delta_3) \tag{35}$$

where $\Delta\alpha_0$, $\Delta V_0'$, and $\Delta\theta_0$ are the magnitudes that the variables would have were they at a maximum at zero time and δ_1, δ_2, and δ_3 are phase angles of the variables with respect to the flight-path angle.

These values of $\Delta\gamma$, $\Delta\alpha$, and $\Delta V'$ may be substituted in equations (12) and solutions made for ζ' and ψ'. It will be found that the complete solution for ζ' and ψ' given in the preceding section can be checked in this manner and the values of $\frac{\Delta\gamma_0}{\Delta\alpha_0}$, $\frac{\Delta\gamma_0}{\Delta V_0'}$, $\tan\delta_1$, and $\tan\delta_2$ are found at intermediate steps to be:

$$\frac{\Delta\gamma_0}{\Delta\alpha_0}=\frac{-\left(C_D\frac{dC_L}{d\alpha}-C_L\frac{dC_D}{d\alpha}+\zeta'\frac{dC_L}{d\alpha}\right)\sin\delta_1}{\psi'(3C_D+4\zeta')}+\frac{\frac{dC_L}{d\alpha}}{(3C_D+4\zeta')}\cos\delta_1 \tag{36}$$

$$\tan\delta_1=\frac{\psi'\left(3C_D+\frac{dC_L}{d\alpha}+4\zeta'\right)}{\left(C_D\frac{dC_L}{d\alpha}-C_L\frac{dC_D}{d\alpha}+\zeta'\frac{dC_L}{d\alpha}\right)-\frac{(3C_D+4\zeta')}{2\zeta'-m_q}\{m_q\zeta'+\mu m_\alpha-[(\zeta')^2-(\psi')^2]\}} \tag{37}$$

$$\frac{\Delta\gamma_0}{\Delta V_0'}=\frac{\left(C_D\frac{dC_L}{d\alpha}-C_L\frac{dC_D}{d\alpha}+\zeta'\frac{dC_D}{d\alpha}\right)}{\psi'\frac{dC_D}{d\alpha}}\sin\delta_2-\frac{\frac{dC_L}{d\alpha}}{\frac{dC_D}{d\alpha}}\cos\delta_2 \tag{38}$$

$$\tan\delta_2=\frac{2\psi'C_L\frac{dC_D}{d\alpha}(2\zeta'-m_q)+\psi'\frac{dC_L}{d\alpha}\,\mathrm{N}}{\left(C_D\frac{dC_L}{d\alpha}-C_L\frac{dC_D}{d\alpha}+\zeta'\frac{dC_L}{d\alpha}\right)\mathrm{N}-2C_L\frac{dC_D}{d\alpha}\left[\mu m_\alpha+\zeta'm_q+(\psi')^2-(\zeta')^2\right]} \tag{39}$$

where

$$\mathrm{N}=-2\mu m_\alpha-4\zeta'm_q-2(\psi')^2+6(\zeta')^2+(2\zeta'-m_q)\left(C_D+\frac{dC_L}{d\alpha}\right)\Big]$$

The detailed derivation is not repeated because it is quite long and tedious and introduces no new concepts.

Application of mathematical formulas.—The relationships derived in the preceding section of this report make possible various treatments of the problem of determining stability. The period and time to damp to one-half amplitude may be determined directly having given C_L, C_D, $\frac{dC_L}{d\alpha}$, $\frac{dC_D}{d\alpha}$, $-m_q$, and $-\mu m_\alpha$ from the equations (17), (24), (25), and either (26) and (27) or (30) and (31).

An understanding of the underlying principles governing stability can be had only from a consideration of the variations of the angle of attack, angle of attitude, angle of flight path, and velocity along the flight path relative to each other. Figures 2 to 14 are included to show the nature of these variations. Figures 2 to 9 present the effects of changing $-m_q$ and $-\mu m_\alpha$ independently for two sets of typical values of C_L, C_D, $\frac{dC_L}{d\alpha}$, and $\frac{dC_D}{d\alpha}$. Figures 10 to 14 illustrate qualitatively the variations in phase relationships resulting from changes in $-\mu m_\alpha$ and serve as a basis for the discussion of their effects upon the stability of the airplane. The relationships (36) to (39) can be used to determine the characteristics of the motion for any particular design.

The solution for the stability characteristics gives no direct indication of the effect of variation of the individual parameters upon the stability characteristics. By means of the relationship that follows directly from equation (22)

$$\begin{aligned}&m_q(c+2\zeta')+\mu m_\alpha-[d+2\zeta'c+4(\zeta')^2]\\&\quad+\left\{\frac{-m_q[d+2\zeta'c+4(\zeta')^2]-\mu m_\alpha(e+2\zeta')+2\zeta'[d+2\zeta'c+4(\zeta')^2]}{-m_q+(c+4\zeta')}\right\}\\&-f\mu m_\alpha\left\{\frac{-m_q+(c+4\zeta')}{-m_q[d+2\zeta'c+4(\zeta')^2]-\mu m_\alpha(e+2\zeta')+2\zeta'[d+2\zeta'c+4(\zeta')^2]}\right\}=0\end{aligned} \tag{40}$$

where

$$c=\frac{1}{2}\left(3C_D+\frac{dC_L}{d\alpha}\right)$$

$$d=\frac{1}{2}\left(C_D\frac{dC_L}{d\alpha}-C_L\frac{dC_D}{d\alpha}+C_R^2\right)$$

$$e=1.5C_D$$

$$f=\frac{1}{2}C_R^2$$

charts may be plotted showing the variations of $-m_q$ with $-\mu m_\alpha$ necessary to secure given values of ζ' and ψ'. A number of these charts have been prepared covering the range of conditions likely to be encountered in normal flight and are included in this report. (See figs. 15 to 54.)

DISCUSSION

The mathematical relationships evolved in the preceding paragraphs permit calculation of the probable stability characteristics of a proposed design, but they offer little information as to the relative importance of various factors or as to the reasons for the effects produced by changes in those factors. In the following paragraphs the oscillatory motion is first considered in detail so that the sequence of flight conditions that must exist if instability is to arise may be pointed out. Next is given a general discussion of charts (figs. 15 to 54) that show the effects on the stability characteristics of the six fundamental parameters C_L, C_D, $\frac{dC_L}{d\alpha}$, $\frac{dC_D}{d\alpha}$, $-\mu m_\alpha$, and $-m_q$. Finally, the effects of various physical characteristics of the airplane on its stability are considered in the light of the earlier discussion.

The oscillatory motion.—When the terms in $\Delta V'$ were eliminated by simultaneous solution of the equations of equilibrium tangent and normal to the flight path, respectively, the following equality was found to exist:

$$\frac{C_D\frac{dC_L}{d\alpha}-C_L\frac{dC_D}{d\alpha}+\lambda'\frac{dC_L}{d\alpha}}{C_R^2+3C_D\lambda'+2(\lambda')^2}=\frac{\mu m_\alpha+m_q\lambda'-(\lambda')^2}{-m_q\lambda'+(\lambda')^2}$$

The terms to the left of the equality sign arise out of the necessity for equilibrium of forces; the terms to the right arise out of the necessity for equilibrium of moments. If a case be investigated with $-\mu m_\alpha=0$

$$C_D\frac{dC_L}{d\alpha}-C_L\frac{dC_D}{d\alpha}+\lambda'\frac{dC_L}{d\alpha}=-C_R^2-3C_D\lambda'-2(\lambda')^2$$

or

$$(\lambda')^2+\frac{1}{2}\left(3C_D+\frac{dC_L}{d\alpha}\right)\lambda'+\frac{1}{2}\left(C_D\frac{dC_L}{d\alpha}-C_L\frac{dC_D}{d\alpha}+C_R^2\right)=0$$

$$\lambda'=-\frac{1}{4}\left(3C_D+\frac{dC_L}{d\alpha}\right)\pm\sqrt{\frac{1}{16}\left(3C_D+\frac{dC_L}{d\alpha}\right)^2-\frac{1}{2}\left(C_D\frac{dC_L}{d\alpha}-C_L\frac{dC_D}{d\alpha}+C_R^2\right)}$$

$$\zeta'=-\frac{1}{4}\left(3C_D+\frac{dC_L}{d\alpha}\right)$$

$$\psi'=\sqrt{\frac{1}{2}\left(C_D\frac{dC_L}{d\alpha}-C_L\frac{dC_D}{d\alpha}+C_R^2\right)-\frac{1}{16}\left(3C_D+\frac{dC_L}{d\alpha}\right)^2}$$

Since both C_D and $\frac{dC_L}{d\alpha}$ are positive below the stall, it follows that if $-\mu m_\alpha$ is zero the linear motion of the airplane is a heavily damped oscillation with the period

$$P'=\frac{2\pi}{\sqrt{\frac{1}{2}\left(C_D\frac{dC_L}{d\alpha}-C_L\frac{dC_D}{d\alpha}+C_R^2\right)-\frac{1}{16}\left(3C_D+\frac{dC_L}{d\alpha}\right)^2}}$$

and the time to damp to one-half amplitude

$$T'=\frac{0.693}{\frac{1}{4}\left(3C_D+\frac{dC_L}{d\alpha}\right)}$$

all in nondimensional units, or the motion is an aperiodic convergence with the time to converge to one-half amplitude

$$T'=\frac{0.693}{\frac{1}{4}\left(3C_D+\frac{dC_L}{d\alpha}\right)\pm\sqrt{\frac{1}{16}\left(3C_D+\frac{dC_L}{d\alpha}\right)^2-\frac{1}{2}\left(C_D\frac{dC_L}{d\alpha}-C_L\frac{dC_D}{d\alpha}+C_R^2\right)}}$$

depending on the relative magnitudes of the quantities.

Since instability of the linear motion cannot arise when $-\mu m_\alpha$ is zero, it seems probable that understanding as to the underlying causes of instability may be gained by considering the effect of $-\mu m_\alpha$ upon the sequence of flight conditions during oscillatory motion. In the following paragraphs the part played by $-\mu m_\alpha$ is analyzed by physical reasoning. Only the case when $-\mu m_\alpha$ is positive is considered because when $-\mu m_\alpha$ is negative an aperiodic divergence from the equilibrium condition occurs and the question of dynamic stability does not arise. It is first pointed out that $-\mu m_\alpha$ plays a primary part in determining the phase angles between the change of angle of attack and the changes in attitude and flight-path angles. It is next shown that stability of the angular motion depends upon the phase angle between the angle-of-attack change and the attitude change. It is finally shown that instability of the linear motion can arise only when the phase angle between the angle-of-attack change and the flight-path-angle change falls within a certain range.

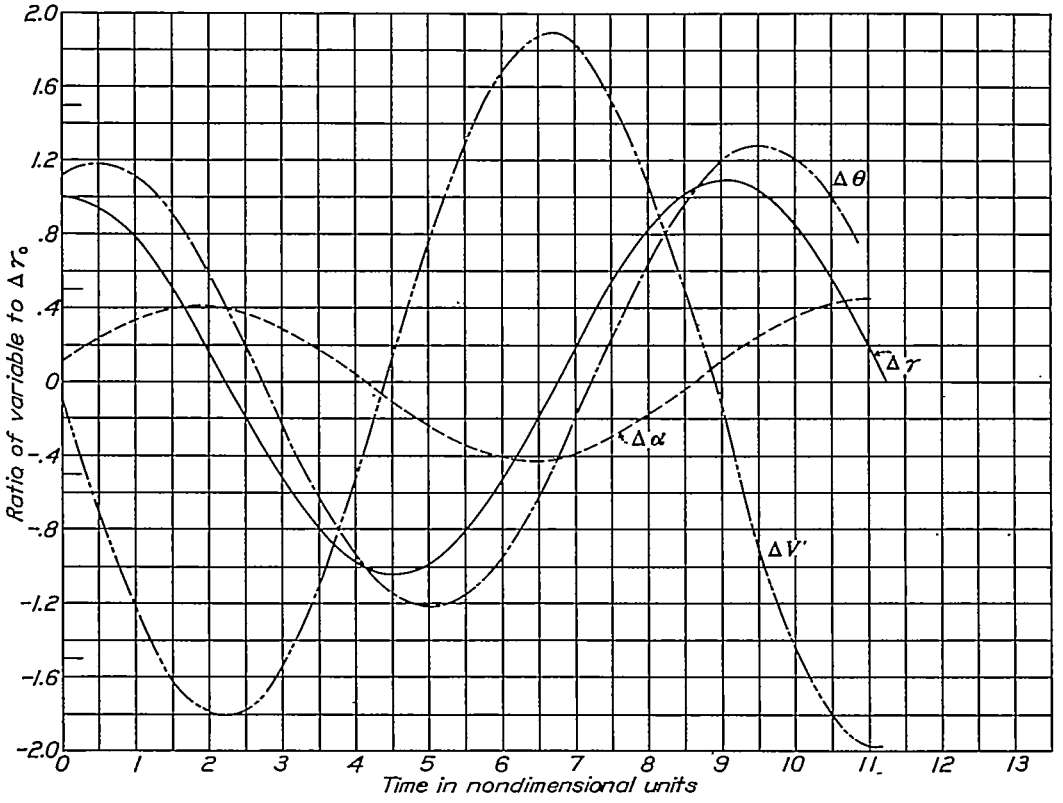

C_L=1.40 C_D=0.20 $\frac{dC_L}{d\alpha}$=4.00 $\frac{dC_D}{d\alpha}$=0.89
$-\mu m_\alpha$=2.50 $-m_q$=1.00 ζ'=0.01 ψ'=0.70

FIGURE 2.

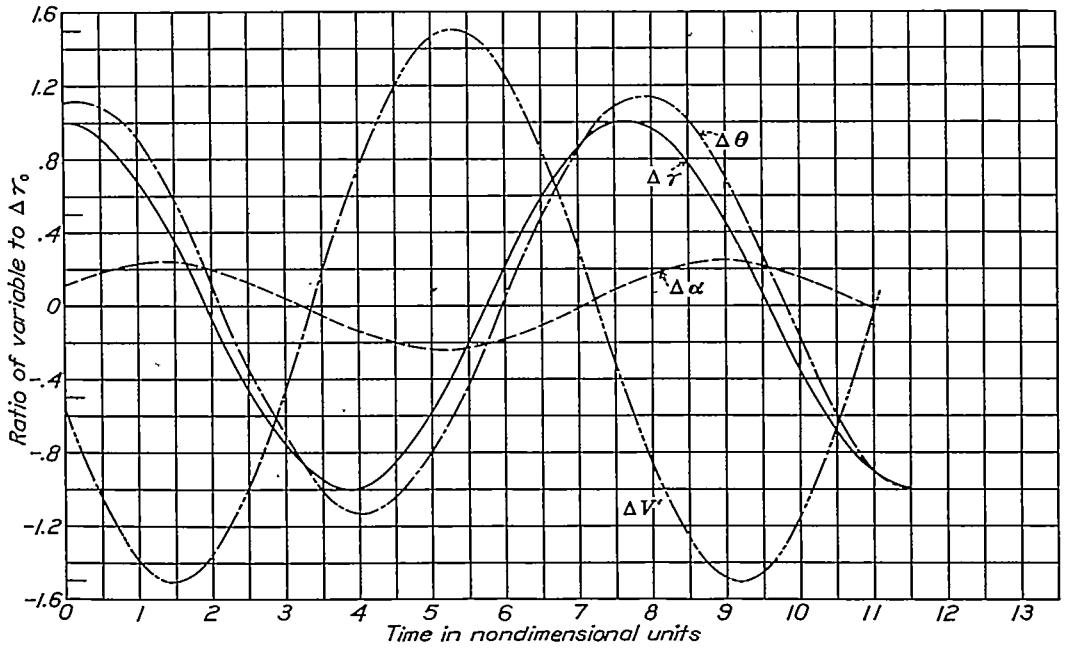

C_L=1.40 C_D=0.20 $\frac{dC_L}{d\alpha}$=4.00 $\frac{dC_D}{d\alpha}$=0.89
$-\mu m_\alpha$=4.94 $-m_q$=1.00 ζ'=0 ψ'=0.82

FIGURE 3.

FIGURES 2 AND 3.—Variations of components of longitudinal motion with time.

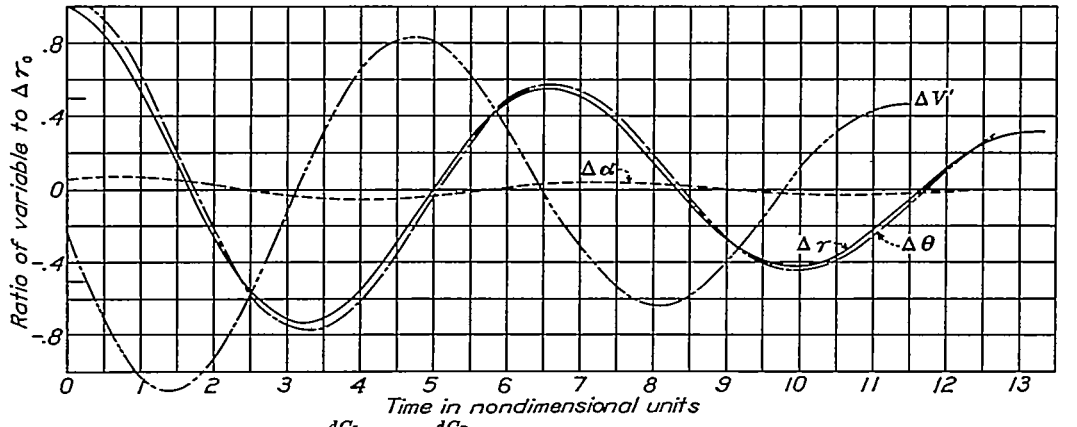

C_L=1.40 C_D=0.20 $\frac{dC_L}{d\alpha}$=4.00 $\frac{dC_D}{d\alpha}$=0.89 $-\mu m_\alpha$=20.00 $-m_q$=1.00 ζ'=−0.09 ψ'=0.94

FIGURE 4.

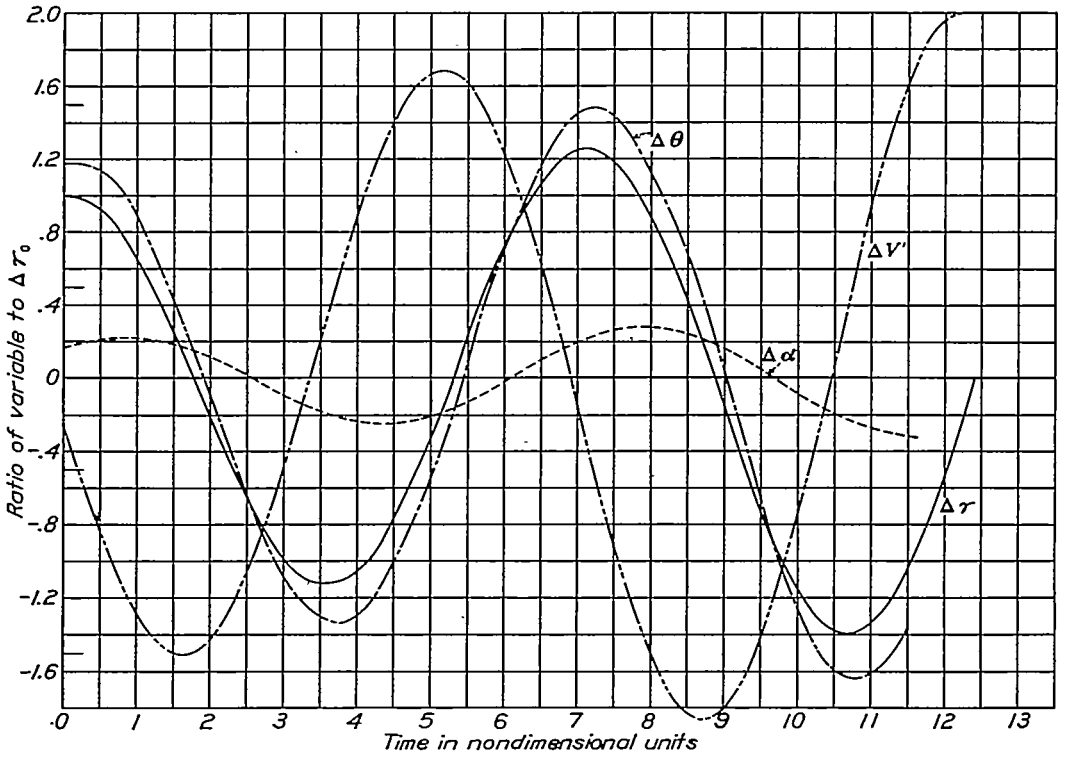

C_L=1.40 C_D=0.20 $\frac{dC_L}{d\alpha}$=4.00 $\frac{dC_D}{d\alpha}$=0.89 $-\mu m_\alpha$=5.00 $-m_q$=0.50 ζ'=0.03 ψ'=0.89

FIGURE E 5.

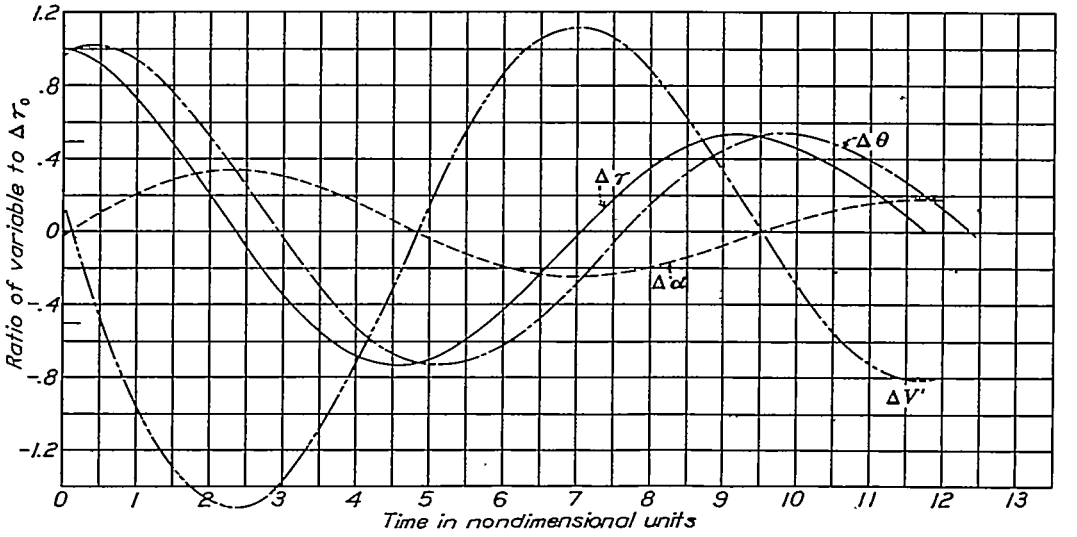

C_L=1.40 C_D=0.20 $\frac{dC_L}{d\alpha}$=4.00 $\frac{dC_D}{d\alpha}$=0.89 $-\mu m_\alpha$=5.00 $-m_q$=3.00 ζ'=−0.07 ψ'=0.67

FIGURE 6.

FIGURES 4, 5, AND 6.—Variations of components of longitudinal motion with time.

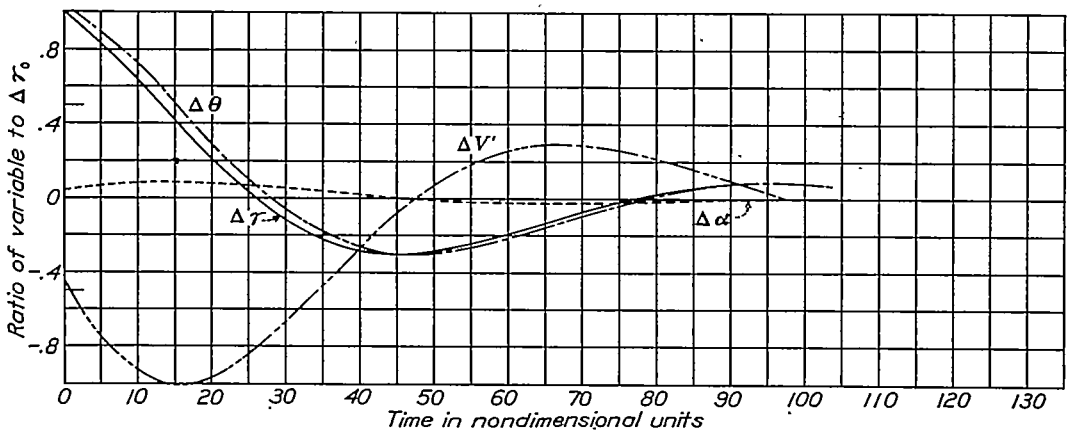

C_L=0.20 C_D=0.043 $\frac{dC_L}{d\alpha}$=4.00 $\frac{dC_D}{d\alpha}$=0.013
$-\mu m_\alpha$=0.54 $-m_q$=1.00 ζ'=−0.025 ψ'=0.061

FIGURE 7.

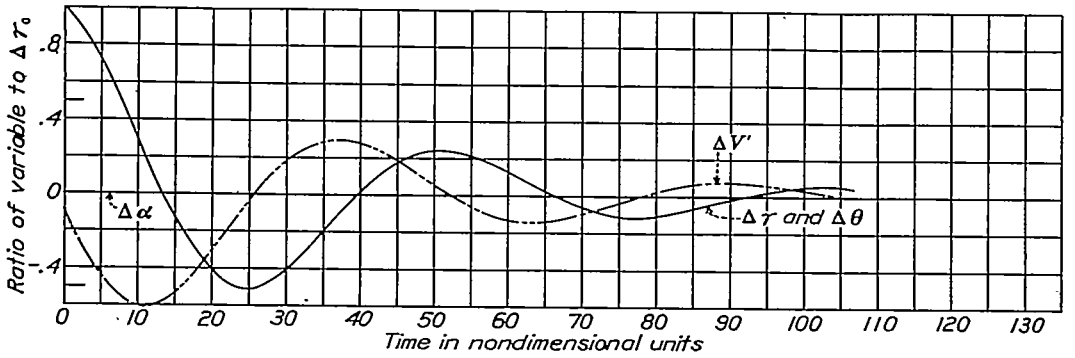

C_L=0.20 C_D=0.043 $\frac{dC_L}{d\alpha}$=4.00 $\frac{dC_D}{d\alpha}$=0.013
$-\mu m_\alpha$=5.00 $-m_q$=1.00 ζ'=−0.028 ψ'=0.12

FIGURE 8.

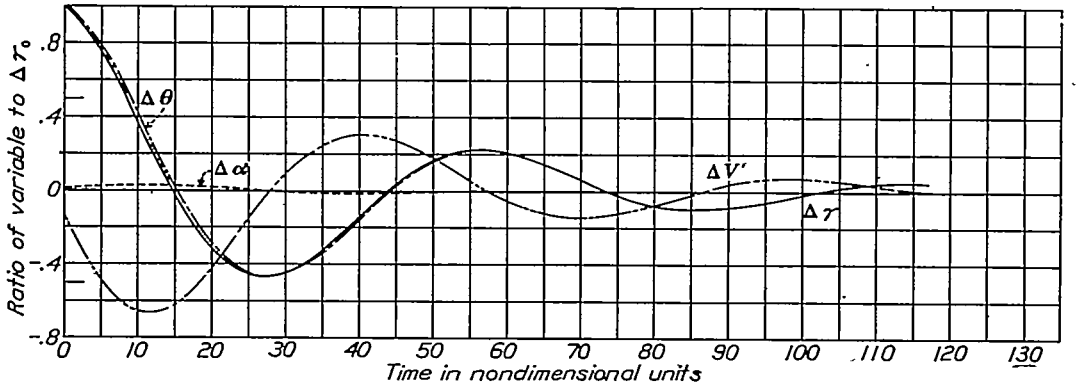

C_L=0.20 C_D=0.043 $\frac{dC_L}{d\alpha}$=4.00 $\frac{dC_D}{d\alpha}$=0.013
$-\mu m_\alpha$=5.00 $-m_q$=3.00 ζ'=−0.027 ψ'=0.11

FIGURE 9.

FIGURES 7, 8, AND 9.—Variations of components of longitudinal motion with time.

Figures 10 to 12 illustrate qualitatively the effect of $-\mu m_\alpha$ upon δ_1 and δ_4, the phase angles between the angle of attack and the flight path and attitude angles, respectively. When $-\mu m_\alpha$ is zero the attitude does not change with time and hence, if an oscillation is set up in the flight-path angle (γ), it is obvious that the angle of attack must change as shown in figure 10 where δ_1 is 180°. Although not shown in figure 10, physical reasoning leads to the conclusion that δ_4 is 90°. When $-\mu m_\alpha$ is very large the moment tending to cause the attitude to change with the flight path is also large and the angle-of-attack change is small. The conditions are approximated by figure 12. The phase angles δ_1 and δ_4 are also small and approach zero as $-\mu m_\alpha$ is increased. Figure 11 shows an intermediate case which more truly represents the usual condition than either of the others. Here $\delta_1<180°$ and $\delta_4<90°$. The curves of figures 10 to 12 were drawn from physical reasoning but are fully confirmed by the computed curves of figures 2 to 4 and 7 and 8.

Referring to the curves of figures 2 to 9 one sees that, if 2 points are chosen exactly 1 period apart when $\Delta\gamma$ is zero, the value of $\Delta V'$ will be found to be greater at the second point than at the first if the motion is unstable, to be unchanged if the motion is neutrally stable, and to be less if the motion is stable. Similar observations can be made with respect to the values of $\Delta\gamma$ when $\Delta V'$ is zero and to the values of $\frac{d\Delta\theta}{dt}$ when $\Delta\theta$ is zero. In other words, when neutral stability exists, the momentum along the average flight path $m(V+\Delta V)$, the momentum perpendicular to the average flight path ($mV\sin\Delta\gamma$), and the angular momentum are each the same at the end of a period as at the beginning. If instability exists, there is more momentum at the end of the period for each of the types of motion than at the beginning. It is therefore desirable to consider the sequence of flight conditions that results in the increase or decrease of momentum in the system.

Consider first the angular motion. Figure 13 is an illustration of a typical set of variations of $\Delta\alpha$, $\Delta\gamma$, and $\Delta\theta$ when ζ' is zero. At the beginning of the half period when $\Delta\theta$ is a maximum, $\Delta q\left(\text{or }\Delta\frac{d\theta}{dt}\right)$ is zero and the angular momentum $B\Delta q$ is therefore zero. At the end of the half period Δq is again zero. It therefore follows that the angular momentum introduced into the system during the half cycle must be balanced by the momentum removed during the same interval.

At each instant when there is a finite value of $\Delta\alpha$, there is a pitching moment introduced into the system equal to $\Delta\alpha\frac{1}{2}\rho V^2Sc\frac{dC_m}{d\alpha}$. Since a moment M applied during a time t introduces angular momentum into the system equal to Mt

$$mk_Y^2\left(\frac{d\theta}{dt}\right)_1=\int_{\psi t=0}^{\psi t=\pi}\Delta\alpha\frac{1}{2}\rho V^2Sc\frac{dC_m}{d\alpha}dt$$
$$=\int_{\psi t=0}^{\psi t=\pi}\frac{1}{2}\rho V^2Sc\frac{dC_m}{d\alpha}\Delta\alpha_0e^{\zeta t}\cos(\psi t-\delta_4)dt$$

represents the angular momentum introduced into the system during one-half cycle (neglecting the effects of terms involving the products of two small quantities, as has been done throughout the discussion).

Considering, for simplicity, the case of neutral stability

$$mk_Y^2\left(\frac{d\theta}{dt}\right)_1=\int_{\psi t=0}^{\psi t=\pi}\frac{1}{2}\rho V^2Sc\frac{dC_m}{d\alpha}\Delta\alpha_0\cos(\psi t-\delta_4)dt$$
$$=\frac{\frac{1}{2}\rho V^2Sc\Delta\alpha_0\frac{dC_m}{d\alpha}}{\psi}\sin(\psi t-\delta_4)\Bigg]_{\psi t=0}^{\psi t=\pi}$$
$$=\frac{\rho V^2Sc\Delta\alpha_0\frac{dC_m}{d\alpha}\sin\delta_4}{\psi}$$

is the angular momentum introduced into the system.

The rotational velocity causes a change of angle of attack at the tail that introduces a moment tending to oppose the rotation. The magnitude of this change is

$$\Delta\alpha=\frac{l\Delta q}{V}=\frac{l\Delta\frac{d\theta}{dt}}{V}=\frac{l\frac{d\theta}{dt}}{V}$$

since

$$\Delta\frac{d\theta}{dt}=\frac{d\theta}{dt}$$

The moment is $-K\eta_t\frac{1}{2}\rho V^2Sl\left(\frac{dC_{z_t}}{d\alpha_t}\frac{S_t}{S}\right)\frac{l\frac{d\theta}{dt}}{V}$. (See p. 3.)

The angular momentum removed from the system ($\zeta=0$) during the half cycle is

$$mk_Y^2\left(\frac{d\theta}{dt}\right)_2=\int_{\psi t=0}^{\psi t=\pi}-K\eta_t\frac{1}{2}\rho VSl^2\left(\frac{dC_{z_t}}{d\alpha_t}\frac{S_t}{S}\right)\psi\Delta\theta_0\sin\psi dt$$
$$=-K\eta_t\rho VSl^2\left(\frac{dC_{z_t}}{d\alpha_t}\frac{S_t}{S}\right)\Delta\theta_0$$

In the case of neutral stability the momentum introduced must equal that removed and therefore

$$\frac{\rho V^2Sc\Delta\alpha_0\frac{dC_m}{d\alpha}\sin\delta_4}{\psi}-\eta_tK\rho VSl^2\left(\frac{dC_{z_t}}{d\alpha_t}\frac{S_t}{S}\right)\Delta\theta_0=0$$

or

$$\frac{\mu m_\alpha}{\psi'}\frac{\Delta\alpha_0}{\Delta\theta_0}\sin\delta_4-m_q=0 \qquad (41)$$

From figures 2, 3, 4, 7, and 8 it is evident that as $-\mu m_\alpha$ increases $\frac{1}{\psi'}$, $\frac{\Delta\alpha_0}{\Delta\gamma_0}$, and δ_4 all decrease. The first term in equation (41) may therefore either increase or decrease with increase in $-\mu m_\alpha$; hence increasing $-\mu m_\alpha$ may decrease the angular momentum added during a cycle. What happens in an actual case depends on the magnitudes of the quantities, as will be brought out later in the discussion.

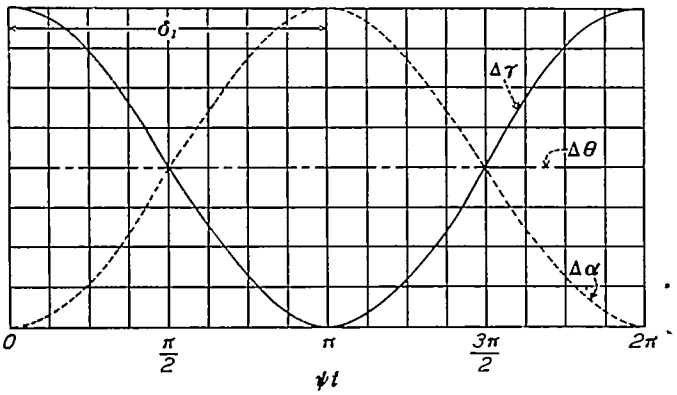

FIGURE 10.—Variations of angle of attack, angle of pitch, and angle of flight path when static stability is zero. Damping coefficient assumed zero.

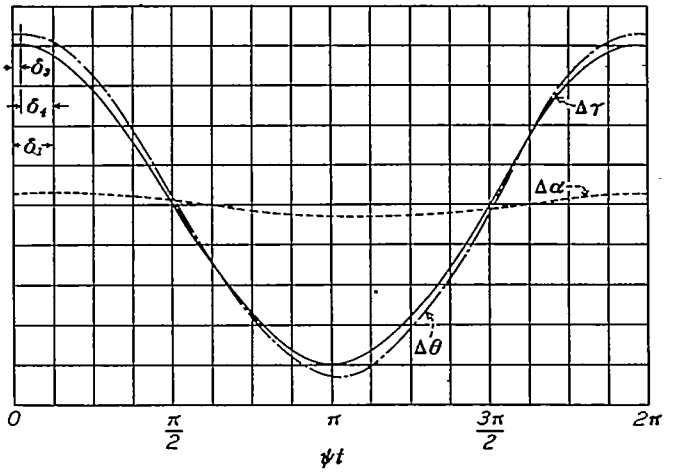

FIGURE 12.—Variations of angle of attack, angle of pitch, and angle of flight path when static stability is great. Damping coefficient assumed zero.

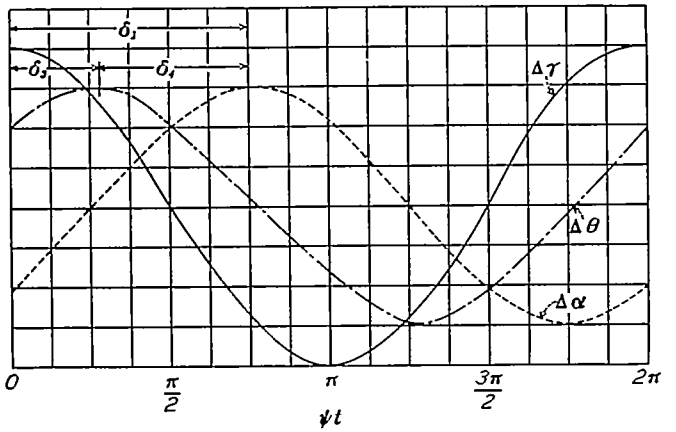

FIGURE 11.—Variations of angle of attack, angle of pitch, and angle of flight path when static stability is small. Damping coefficient assumed zero.

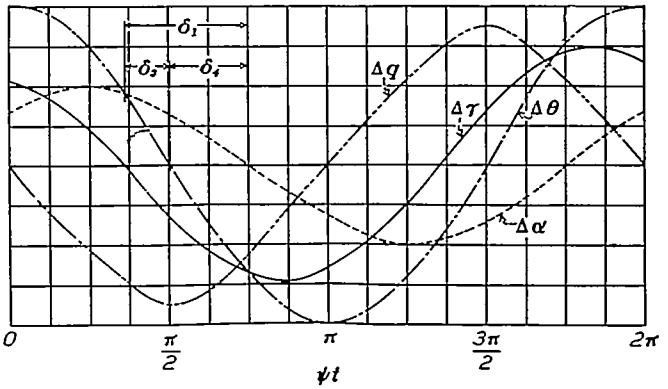

FIGURE 13.—Variations of angle of attack, angle of flight path, rotational velocity, and angle of pitch for an illustrative case. Damping coefficient assumed zero.

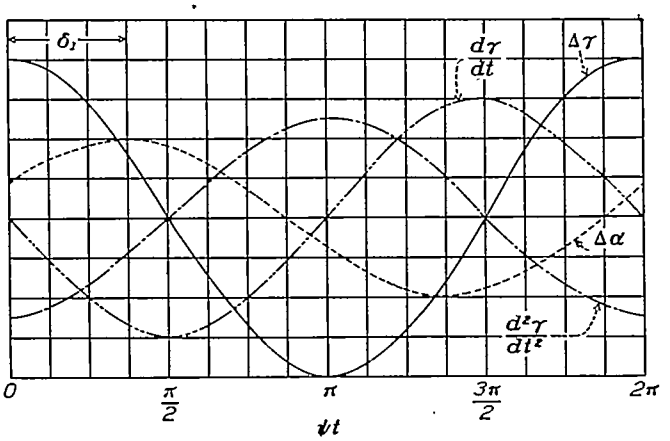

FIGURE 14.—Variations of angle of attack, rate of change of angle of flight path, and angle of flight path for an illustrative case. Damping coefficient assumed zero.

The introduction of linear momentum along and perpendicular to the flight path might be discussed by considering equations (12a) and (12b) separately but the analysis may be simplified by combining the two through elimination of terms involving $\Delta V'$ and $\frac{dV'}{dt}$. The relationship established is:

$$-C_R^2\Delta\gamma-3C_D\tau\frac{d\gamma}{dt}-2\tau^2\frac{d^2\gamma}{dt^2}= -\left(C_D\frac{dC_L}{d\alpha}-C_L\frac{dC_D}{d\alpha}\right)\Delta\alpha-\tau\frac{dC_L}{d\alpha}\frac{d\alpha}{dt}$$

Considering the case of zero damping during the interval from $\psi t=0$ to $\psi t=\pi$ it is obvious from figure 14 that the integral sum of terms multiplied by $\Delta\gamma$ or by $\frac{\Delta^2\gamma}{dt^2}$ is zero because these quantities are symmetrical with respect to the zero line. The equation of equality of momentum introduced to that removed becomes:

$$\int_{\psi t=0}^{\psi t=\pi}-3C_D\tau\frac{d\gamma}{dt}dt=\int_{\psi t=0}^{\psi t=\pi}-\left(C_D\frac{dC_L}{d\alpha}-C_L\frac{dC_D}{d\alpha}\right)\Delta\alpha dt - \int_{\psi t=0}^{\psi t=\pi}\tau\frac{dC_L}{d\alpha}\frac{d\alpha}{dt}dt$$

which reduces to

$$-3C_D-\frac{\left(C_D\frac{dC_L}{d\alpha}-C_L\frac{dC_D}{d\alpha}\right)}{\psi'}\frac{\Delta\alpha_0}{\Delta\gamma_0}\sin\delta_1+\frac{dC_L}{d\alpha}\frac{\Delta\alpha_0}{\Delta\gamma_0}\cos\delta_1=0 \quad (42)$$

The growth of linear momentum therefore depends upon δ_1, $\frac{\Delta\alpha_0}{\Delta\gamma_0}$, and ψ' in addition to the parameters C_D, C_L, $\frac{dC_D}{d\alpha}$, and $\frac{dC_L}{d\alpha}$. Since $\frac{\Delta\alpha_0}{\Delta\gamma_0}$ is normally positive the following facts appear: C_D is a factor serving always to remove momentum from the system; $\left(C_D\frac{dC_L}{d\alpha}-C_L\frac{dC_D}{d\alpha}\right)\frac{1}{\psi'}$ is a factor adding energy to the system when $C_L\frac{dC_D}{d\alpha}>C_D\frac{dC_L}{d\alpha}$, as is normally the case at high angles of attack; and $\frac{dC_L}{d\alpha}$ adds momentum to the system when $\delta_1<90°$ and removes momentum when $\delta_1>90°$. When $-\mu m_\alpha$ is zero, $\delta_1=180°$ and the factor removing energy from the system is $\left(3C_D+\frac{dC_L}{d\alpha}\right)$, as was shown earlier in the discussion. As $-\mu m_\alpha$ is increased, δ_1, $\frac{\Delta\alpha_0}{\Delta\gamma_0}$, and $\frac{1}{\psi'}$ all decrease (figs. 2, 3, 4, 7, and 8). The factor $\left(C_D\frac{dC_L}{d\alpha}-C_L\frac{dC_D}{d\alpha}\right)\frac{1}{\psi'}\frac{\Delta\alpha_0}{\Delta\gamma_0}\sin\delta_1$ reaches its maximum at some point between $\delta_1=180°$ and $\delta_1=90°$. The factor $\frac{dC_L}{d\alpha}\frac{\Delta\alpha_0}{\Delta\gamma_0}\cos\delta_1$ changes from a stabilizing to an unstabilizing influence at $\delta_1=90°$ and reaches a maximum as an unstabilizing element between $\delta_1=90°$ and $\delta_1=0$. It would appear at first thought that the effect of $\frac{dC_L}{d\alpha}$ as an unstabilizing factor would always be small because of the decrease of $\frac{\Delta\alpha_0}{\Delta\gamma_0}$ with increase of $\cos\delta_1$ but such is not necessarily the case because of the large ratio of $\frac{dC_L}{d\alpha}$ to C_D, particularly at low angles of attack.

There is an interesting point in connection with the factor $\left(C_D\frac{dC_L}{d\alpha}-C_L\frac{dC_D}{d\alpha}\right)$ that appears as the chief unstabilizing element at small values of $-\mu m_\alpha$. If the law of induced drag be applied to determine C_D and $\frac{dC_D}{d\alpha}$, it appears that

$$\left(C_D\frac{dC_L}{d\alpha}-C_L\frac{dC_D}{d\alpha}\right)=C_{D_p}\frac{dC_L}{d\alpha}+C_{D_i}\frac{dC_L}{d\alpha}-C_L\frac{dC_{D_i}}{d\alpha}$$

$$=C_{D_p}\frac{dC_L}{d\alpha}+\frac{C_L^2\frac{dC_L}{d\alpha}}{\frac{b^2}{\pi S}}-C_L\frac{2C_L\frac{dC_L}{d\alpha}}{\frac{b^2}{\pi S}}$$

$$=\frac{dC_L}{d\alpha}\left(C_{D_p}-\frac{C_L^2}{\frac{b^2}{\pi S}}\right)$$

$$=\frac{dC_L}{d\alpha}(C_{D_p}-C_{D_i})$$

Therefore equation (42) may be rewritten as

$$-3C_D+\frac{dC_L}{d\alpha}\frac{\Delta\alpha_0}{\Delta\gamma_0}\left[(C_{D_i}-C_{D_p})\frac{1}{\psi'}\sin\delta_1+\cos\delta_1\right]=0 \quad (43)$$

It appears that instability of the linear motion for small values of $-\mu m_\alpha$ can occur only at angles of attack where $C_{D_i}>C_{D_p}$. The detrimental effect of C_{D_i} is not as great as at first appears, however, because the damping factor 3 C_D increases with C_{D_i} also.

In the foregoing analysis, the effect of ζ' has been neglected and therefore the statements made cannot be considered rigorously true when the stability or instability is of appreciable magnitude. The analysis does, however, point out the more important influences and the nature of the interaction of events that brings them into play. Equation (43) cannot be applied near the stall where $\frac{dC_D}{d\alpha}$ ceases to equal $\frac{2C_L\frac{dC_L}{d\alpha}}{\frac{b^2}{\pi S}}$.

In figures 2 to 14, inclusive, and in the discussion of the oscillatory motion an arbitrary value of $\Delta\gamma_0=1$ has been assumed. No attempt will be made to evaluate $\Delta\gamma_0$ in terms of control movements or gust velocities as the actual magnitude is unimportant with respect to stability (assuming that the deviations are not so great as to destroy the validity of the basic assumptions). It seems not out of place, however, to suggest that relative magnitudes of $\frac{\Delta\alpha_0}{\Delta\gamma_0}$ $\frac{\Delta V_0'}{\Delta\gamma_0}$ $\frac{\Delta\theta_0}{\Delta\gamma_0}$, δ_1, δ_2, etc.,

may have important bearing upon the comfort, ease of handling, and design load factor of aircraft and that further work taking these factors into consideration might lead to valuable information.

Charts of rotational damping factor against static stability factor.—In the section dealing with application of mathematical formulas a convenient graphical means of showing the variation of ζ' and ψ' with $-m_q$ and $-\mu m_\alpha$ has been described. This method of presentation was given by Gates (reference 5) in essentially the same fashion although differing in detail. In reference 5 preference is given to charts with coordinates of tail volume and fore-and-aft location of the center of gravity. Preference has been given in this report to charts with coordinates of rotational damping factor and static-stability factor because they are more convenient for use with data from wind-tunnel tests, they do not require assumption of arbitrary fixed values for several important factors, and they cover a much wider range for a given number of charts. The charts are entirely nondimensional and vary only with C_L, C_D, $\frac{dC_L}{d\alpha}$, and $\frac{dC_D}{d\alpha}$. Variation of empirical factors such as the K in $-m_q$, η_t, $\frac{d\alpha_t}{d\alpha}$ (see p. 17), etc., affect only $-m_q$ or $-\mu m_\alpha$, as the case may be, and their effects upon the stability are readily apparent.

The series of charts presented (figs. 15 to 54) are intended to show somewhat more precisely and completely than has been done in the preceding discussion the effects of the parameters C_L, C_D, $\frac{dC_L}{d\alpha}$, and $\frac{dC_D}{d\alpha}$ upon dynamic stability and to provide a convenient graphical means by which the designer may estimate the probable stability characteristics of a proposed airplane and the effects of various changes without recourse to extensive calculations. The charts cover the range of values of the parameters that appear likely to be attained in the near future. The values represented are summarized in table I.

Certain general characteristics of the charts are immediately apparent upon inspection. As $-\mu m_\alpha$ increases from zero, ζ' at first becomes more positive corresponding to a decrease in dynamic stability but, at a fairly small value of $-\mu m_\alpha$, changes its trend and becomes more negative. This tendency is general throughout all the charts and is apparent whether $-m_q$ is large or small. It will be remembered that such an effect appeared probable from the discussion of the introduction of angular momentum into the system during a cycle by $-m_\alpha$. As pointed out at that stage of the report, $\frac{\Delta\alpha_0}{\Delta\gamma_0}$, $\sin\delta_4$, and $\frac{1}{\psi'}$, all decrease with increase of $-\mu m_\alpha$; the charts of variation of the stability characteristics with $-m_q$ and $-\mu m_\alpha$ show definitely that the decrease of the product of these factors is much more than sufficient to nullify the increases in $-\mu m_\alpha$ after a certain value of $-\mu m_\alpha$ has been exceeded. Increase of ψ', hence decrease in period of the oscillations, with increase of $-\mu m_\alpha$ occurs at practically all values of $-m_q$ and $-\mu m_\alpha$.

Increases of $-m_q$ give, in general, more negative values of ζ' and consequently more rapid dying out of the oscillations. At large values of $-\mu m_\alpha$ increases in $-m_q$ give more positive values of ζ' but this effect is not of practical importance. It will be noticed that at fairly large values of $-\mu m_\alpha$ increasing $-m_q$ has but slight effect but that $-m_q$ becomes of increasing importance as $-\mu m_\alpha$ is made smaller. Increasing $-m_q$ decreases ψ' rather gradually, giving oscillations of longer period. It appears that if the criterion of stability be taken as the number of oscillations necessary for the amplitude to decrease to one-half its original value then the value of $-m_q$ is of particular importance.

The charts of figures 23, 27, 28, and 29 show that increasing C_L without changing other factors increases quite markedly the tendency to instability. This observation agrees well with the effect to be expected from increasing C_L that might have been predicted from the part played by C_L in the factor $\left(C_D\frac{dC_L}{d\alpha}-C_L\frac{dC_D}{d\alpha}\right)$ in equation (42).

The effect of increasing C_D without changing other factors appears in figures 29, 30, and 31. It will be seen that increasing C_D reduces the range of instability and brings the curves of $\zeta'=k$ nearer together with a very large net increase in damping. The effect upon ψ' is negligible.

The slope of the lift curve is of importance although not giving such extreme effects as changes in C_L and C_D (figs. 34, 35, and 36). Here again the effect is in good agreement with equation (42). Increasing $\frac{dC_L}{d\alpha}$ tends to extend the instability region to greater values of $-\mu m_\alpha$ or, in other words, if $-\mu m_\alpha$ is large, δ_1 is less than 90° and $\frac{dC_L}{d\alpha}$ becomes a definite unstabilizing factor. At small values of $-m_\alpha$, $\frac{dC_L}{d\alpha}$ is a stabilizing factor, as is apparent from the curves. Increasing $\frac{dC_L}{d\alpha}$ also tends to decrease ψ'.

Increasing the slope of the drag curve is distinctly unfavorable to stability as shown in figures 42, 44, and 45. The period of the oscillation is but slightly affected.

Reference to charts 15, 21, and 33 shows that the general effect of increasing angle of attack is to increase the region of instability but to decrease the spread between curves of $\zeta'=k$. It appears that instability of the oscillatory motion is very unlikely for small angles of attack and becomes increasingly likely with increase of that angle. On the other hand, if $-\mu m_\alpha$ and $-m_q$ remain unchanged throughout the change of angle of attack, the value of ζ' may become more negative, which seems to be directly contradictory to the preceding statement. The explanation

lies in the fact that at small angles of attack changes of $-\mu m_\alpha$ and $-m_q$ have little effect upon the damping coefficient; whereas at large angles of attack a small change in $-\mu m_\alpha$ or $-m_q$ may change the damping coefficient from a definite negative value to a definite positive value. The period of the oscillation decreases markedly with the increase of angle of attack but the decrease is not so great as would appear to be the case from consideration of the increase in ψ'. The period in seconds is proportional to $\frac{\sqrt{C_L}}{\psi'}$ and the increase in C_L is sufficiently great partly to counteract the increase in ψ'.

The effects of various physical characteristics of the airplane on the stability.—In the preceding discussion no consideration has been given to the various dimensional characteristics, aerodynamic interferences, etc., that determine the values of the fundamental parameters. A large number of factors affect the stability but in many cases the effects are of a minor nature. Only the more important ones will be discussed in the following paragraphs.

The wing loading appears in but two places in the analysis of stability in this report. The nondimensional relative-density factor

$$\mu=\frac{m}{\rho S l}=\frac{\frac{W}{S}}{32.2\,\rho l}=\frac{13.1\left(\frac{W}{S}\right)}{l}$$ (standard conditions at sea level)

is directly proportional to wing loading and the factor $\tau=\frac{m}{\rho S V}=\frac{\sqrt{\frac{W}{S}C_L}}{2.22}$ is proportional to the square root of wing loading. Since μ appears only as the coefficient of $-m_\alpha$ it is apparent that the variation of the nondimensional values of ζ' and ψ' with μ are the same as for variations of $-\mu m_\alpha$. It therefore appears that, if the longitudinal motion of an airplane with respect to the air is to be unaffected, an increase in the wing loading of a given design must be accompanied by a proportional decrease in $\frac{dC_m}{d\alpha}$ provided that l, c, and k_Y are unchanged. Aside from the effect upon $-\mu m_\alpha$ the wing loading affects the stability characteristics through the time factor τ, which appears in the reduction of the nondimensional units ζ' and ψ' to the time to damp to one-half amplitude and to the period of the oscillation in seconds

$$T=\frac{-0.693}{\zeta'}\tau$$

and

$$P=\frac{2\pi}{\psi'}\tau$$

If $-\mu m_\alpha$ is preserved unchanged as $\frac{W}{S}$ is increased, both the period and the time to damp are increased but the number of oscillations for a given degree of damping is unchanged. The effect of an increase of wing loading without change of other factors is therefore to increase both ψ' and τ with the net effect, in general, of increasing the period; to make ζ' more negative if $-\mu m_\alpha$ is large, with a net effect upon the time to damp either of an increase or of a decrease; and to make ζ' less negative if $-\mu m_\alpha$ is small, resulting in a comparatively large net increase in the time to damp to one-half amplitude.

The aspect ratio of the wing combination affects the stability indirectly through its effect upon the parameters $\frac{dC_L}{d\alpha}$, $\frac{dC_D}{d\alpha}$, and C_D at a given value of C_L. Increasing the aspect ratio increases $\frac{dC_L}{d\alpha}$ and decreases both $\frac{dC_D}{d\alpha}$ and C_D. Comparison of the curves of figures 36 and 39 corresponding to aspect ratios of 5 and 8, respectively, shows that (neglecting the effect due to change of $\frac{dC_L}{d\alpha}$, which is comparatively small and will not materially affect the conclusions to be drawn) the net effect of increasing the aspect ratio is to increase the range of instability. The decrease in $\frac{dC_D}{d\alpha}$, an effect favorable to stability, is less important than the decrease in C_D, which quite markedly tends to decrease the stability.

The effect of parasite drag is brought out quite clearly in figures 33, 36, and 40. (In general, increasing the parasite drag also increases the slope of the drag curve and this fact has been taken into account in the figures by using the method of reference 6.) It is apparent that the drag is an important item in determining the stability characteristics of a design and that the "cleaner" the airplane the greater the tendency to unstable oscillations. Increasing the parasite drag results in a decrease in the unstabilizing factor $(C_{D_i}-C_{D_p})$ and an increase in the stabilizing factor $3C_D$, which appears in equation (42) in the discussion of the growth of linear momentum during a cycle. It appears therefore that air brakes of various kinds may be expected to have beneficial effects upon the longitudinal stability provided that they do not introduce undesirable moments or interferences. Highly efficient designs that achieve high values of $C_{L_{max}}$ without the use of devices introducing parasite drag may be expected to be deficient in longitudinal damping.

The moment of inertia of the airplane about the lateral axis appears as the term k_Y^2 in the denominators of the expressions for $-m_q$ and $-m_\alpha$. Increasing k_Y^2 decreases both $-m_q$ and $-\mu m_\alpha$ proportionally with a corresponding increase in the time to damp. The

effect may be readily visualized by imagining any point $-\mu m_\alpha$, $-m_q$ upon the chart moved from or toward the origin along a radial line an amount such that the ratio of the new distance to the origin to the original distance is the ratio of the original value of k_Y^2 to the new value. It is therefore to be expected that distribution of the mass of an airplane along its longitudinal axis may lead to unstable oscillations although other factors such as length and size of tail, location of the center of gravity, etc., are such that ordinarily the damping would be satisfactory. The effect upon the period of changing k_Y^2 is not great although increasing k_Y^2 will, in general, lead to oscillations of shorter period.

The location of the center of gravity affects the longitudinal stability through its effect upon the term $\frac{dC_m}{d\alpha}$ appearing in the expression for $-m_\alpha$. The pitching moment of an airplane about the center of gravity may be expressed as

$$C_{m_{c.g.}}=-C_{z_w}(C_g-C_a)+C_{m_{0_w}}+C_{x_w}\frac{z}{c}+C_{m_p}+\alpha_t\frac{dC_{z_t}}{d\alpha_t}\frac{l}{c}\frac{S_t}{S}\eta_t$$

Differentiating with respect to angle of attack

$$\frac{dC_m}{d\alpha}=\frac{-dC_{z_w}}{d\alpha}(C_g-C_a)+\frac{dC_{x_w}}{d\alpha}\frac{z}{c}+\frac{dC_{m_p}}{d\alpha}+\frac{d\alpha_t}{d\alpha}\frac{dC_{z_t}}{d\alpha_t}\frac{l}{c}\frac{S_t}{S}\eta_t$$

or, for practical purposes,

$$\frac{dC_m}{d\alpha}=\frac{dC_L}{d\alpha}(C_g-C_a)+\frac{dC_{x_w}}{d\alpha}\frac{z}{c}+\frac{dC_{m_p}}{d\alpha}+\eta_t\frac{d\alpha_t}{d\alpha}\frac{dC_{z_t}}{d\alpha_t}\frac{l}{c}\frac{S_t}{S}$$

where

C_g, ratio of distance of c. g. from the leading edge of the wing to the wing chord.

C_a, ratio of the distance of the aerodynamic center of the wing from the leading edge of the wing to the wing chord.

C_{z_w}, normal-force coefficient of wing.

C_{x_w}, longitudinal-force coefficient of wing.

z, distance of mean wing chord below c. g.

C_{m_p}, parasite pitching-moment coefficient of fuselage and landing gear.

$\frac{d\alpha_t}{d\alpha}$, ratio of change of angle of attack at the tail to change of angle of attack at the wing, an empirical factor depending upon downwash (reference 7).

Since $\frac{dC_L}{d\alpha}$ is positive, increasing C_g by moving the center of gravity toward the rear tends to make $\frac{dC_m}{d\alpha}$ less negative and to decrease $-\mu m_\alpha$. The effect of longitudinal center-of-gravity location upon the stability characteristics thus follows from the preceding discussion of the effect of changes in $-\mu m_\alpha$. The location of the aerodynamic center of the wing, defined by C_a, affects the stability in the same manner as the location of the center of gravity but with the opposite sign. The value of C_a given by wing theory is 0.25 (reference 8). Wind-tunnel data indicate the actual values to range from 0.23 to 0.25 for conventional airfoils (reference 9).

The vertical location of the center of gravity with respect to the mean aerodynamic wing chord is not unimportant in many cases and should be considered particularly in high-wing or low-wing monoplanes. Since $\frac{dC_{x_w}}{d\alpha}$ is positive, positive values of $\frac{z}{c}$ (as in the case of a low-wing monoplane) make $\frac{dC_m}{d\alpha}$ less negative and may cause an unstable divergence (static instability) in cases that would be considered stable on the basis of calculations involving only C_g. The value of $\frac{dC_{x_w}}{d\alpha}$ is derived as follows:

$$C_{x_w}=-C_{D_w}\cos\alpha+C_L\sin\alpha$$

$$\frac{dC_{x_w}}{d\alpha}=\left(C_L-\frac{dC_{D_w}}{d\alpha}\right)\cos\alpha+\left(C_{D_w}+\frac{dC_L}{d\alpha}\right)\sin\alpha$$

where C_{D_w} and $\frac{dC_{D_w}}{d\alpha}$ are for the wing alone. For a case with $C_L=1.4$, $\frac{dC_L}{d\alpha}=4$, $C_{D_{0_w}}=0.01$, $\frac{b^2}{S}=6$, $\alpha=15°$

$$C_{D_w}=0.01+\frac{C_L^2}{6\pi^2}=0.11$$

$$\frac{dC_{D_w}}{d\alpha}=\frac{2\times1.4\times4}{6\pi^2}=0.60$$

$$\frac{dC_{x_w}}{d\alpha}=(0.8\times0.966)+(4.11\times0.259)$$

$$0.77+1.06=1.83$$

Assuming the case of a low-wing monoplane with $\frac{z}{c}=0.25$ and $C_g=0.30$, it will be found that the stability will be the same as though

$$\frac{z}{c}=0 \text{ and } C_g=0.30+\left(\frac{1.83}{4}\times0.25\right)=0.41.$$

The example represents perhaps an extreme case but illustrates the desirability of investigating the effect of vertical center-of-gravity location.

The value of the slope of the curve of parasite pitching-moment coefficient against angle of attack may be determined with reasonable accuracy only by careful testing of a scale model or the complete airplane. For a number of designs of military airplanes for which sample computations were made and compared with measured values of $\frac{dC_{m_{c.g.}}}{d\alpha}$ values of $\frac{dC_{m_p}}{d\alpha}$ were found to range from 0 to 0.4, with an average value of 0.2, at angles of attack corresponding to cruising and high speeds. The value of $\frac{dC_{m_p}}{d\alpha}$ became

less positive as the angle of attack was increased in all cases where it was of appreciable magnitude but in no case became negative. It therefore appears that the parasite pitching moment will be, in general, such as to decrease $-\mu m_\alpha$ with corresponding effects upon the stability characteristics.

The tail length, size, and aspect ratio are very important factors in the stability characteristics. Tail length appears both in $-m_q$ and in $-\mu m_\alpha$. It will be remembered that

$$-m_q=-K\eta_t\frac{l^2}{2k_Y^2}\frac{S_t}{S}\frac{dC_{z_t}}{d\alpha_t}$$

$$-\mu m_\alpha=-\frac{m}{\rho Sl}\frac{lc}{2k_Y^2}\left[\frac{dC_L}{d\alpha}(C_q-C_a)+\frac{dC_X}{d\alpha}\frac{z}{c}+\frac{dC_{m_p}}{d\alpha}+\eta_t\frac{d\alpha_t}{d\alpha}\frac{dC_{z_t}}{d\alpha_t}\frac{S_t}{S}\frac{l}{c}\right]$$

Increasing l has a very beneficial effect upon the factor $-m_q$, which is proportional to the square of l. In an actual case increasing l will also increase k_Y, and perhaps in some cases η_t, so that the net increase in $-m_q$ will only approximate that indicated by considering only the square of the tail length. Increasing l makes $-\mu m_\alpha$ larger because of the increase in moment arm of the tail. There are also secondary effects because l affects $\frac{d\alpha_t}{d\alpha}$, η_t, and k_Y. The net effect of small increases in tail length can only be predicted from consideration of the particular design. There is a small range of conditions, corresponding to small values of $-\mu m_\alpha$, in which increasing l increases the time to damp because the effect upon $-\mu m_\alpha$ is of more importance than the increase in $-m_q$. Large increases in l will always increase the period and decrease the time to damp.

It has been mentioned that l affects η_t and $\frac{d\alpha_t}{d\alpha}$. The effect upon η_t is small and may be neglected. Increasing tail length increases $\frac{d\alpha_t}{d\alpha}$. The angle of attack at the tail may be expressed as

$$\alpha_t=\alpha+i_t-\epsilon$$

where i_t is the incidence of the tail referred to the wing chord.

The downwash may be expressed as

$$\epsilon=\frac{60}{R}(x+1)^{-0.38}(y+1)^{-0.23}C_L \text{ (reference 10)}$$

where R is the equivalent monoplane aspect ratio of the wing combination and x and y are the distances of the tail plane behind and above or below the trailing edge of the wing in chord lengths. The value ϵ therefore decreases exponentially with tail length and hence

$$\frac{d\alpha_t}{d\alpha}=1-\frac{d\epsilon}{d\alpha}$$

$$=1-K\frac{dC_L}{d\alpha}$$

becomes greater with increase of l.

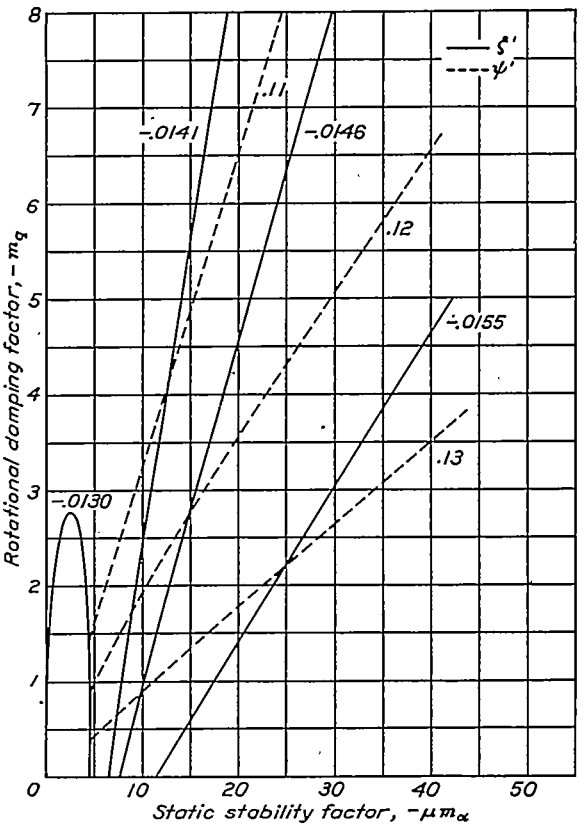

C_L=0.20 $\frac{dC_L}{d\alpha}$=4.00 C_D=0.023 $\frac{dC_D}{d\alpha}$=0.11

FIGURE 15.

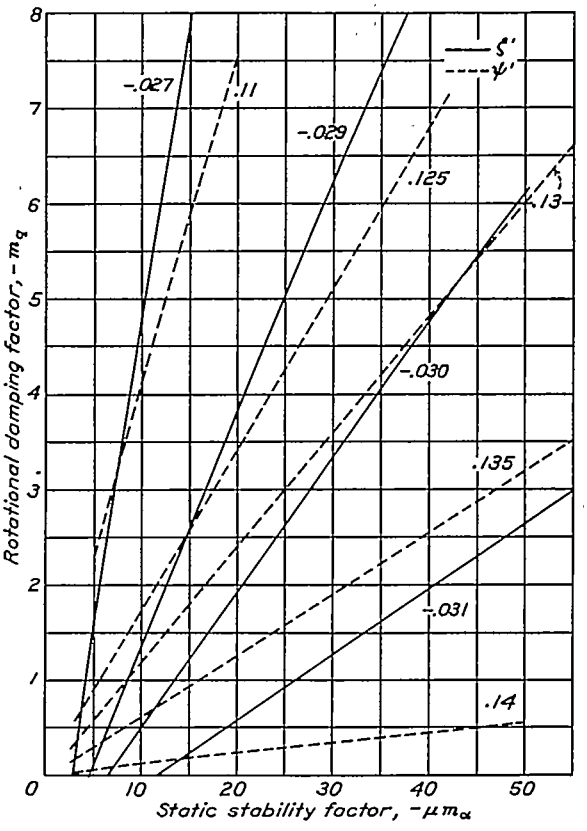

C_L=0.20 $\frac{dC_L}{d\alpha}$=3.00 C_D=0.043 $\frac{dC_D}{d\alpha}$=0.10

FIGURE 16.

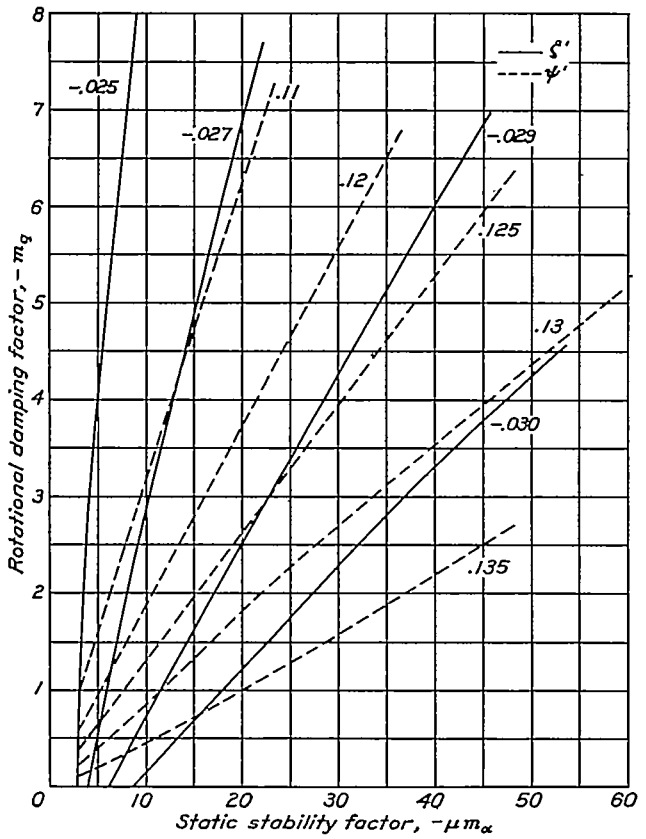

C_L=0.20 C_D=0.043
$\frac{dC_L}{d\alpha}$=4.00 $\frac{dC_D}{d\alpha}$=0.13

FIGURE 17.

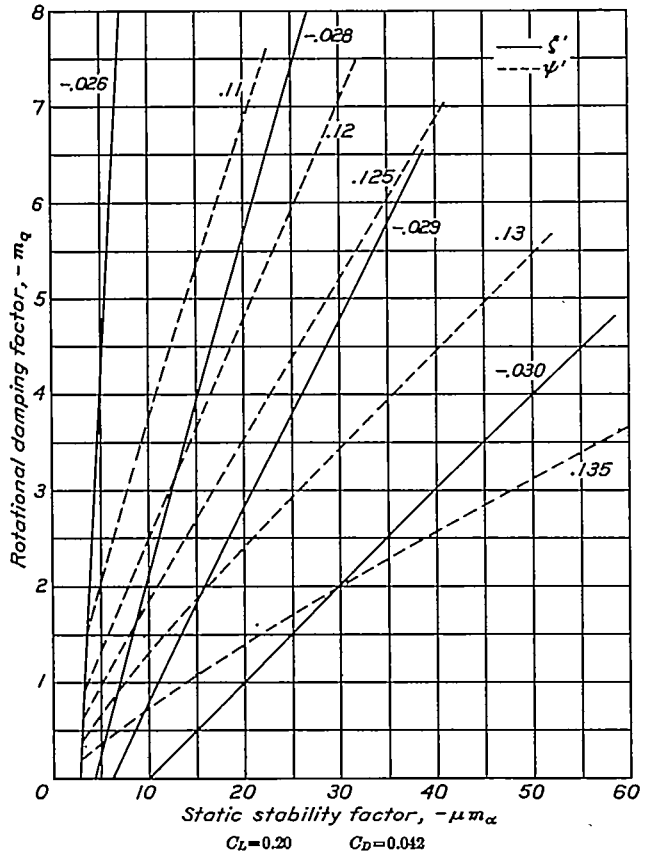

C_L=0.20 C_D=0.042
$\frac{dC_L}{d\alpha}$=3.00 $\frac{dC_D}{d\alpha}$=0.06

FIGURE 18.

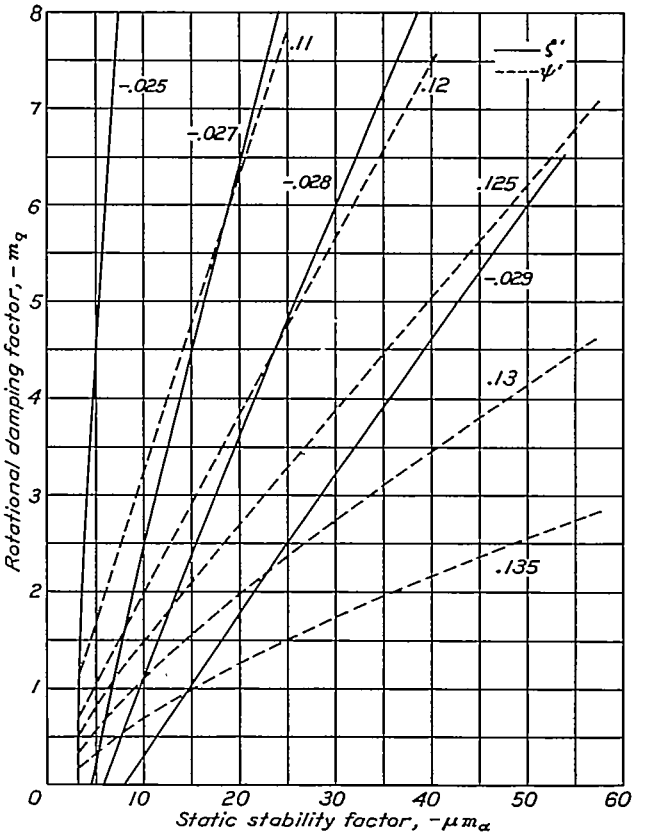

C_L=0.20 C_D=0.042
$\frac{dC_L}{d\alpha}$=4.00 $\frac{dC_D}{d\alpha}$=0.08

FIGURE 19.

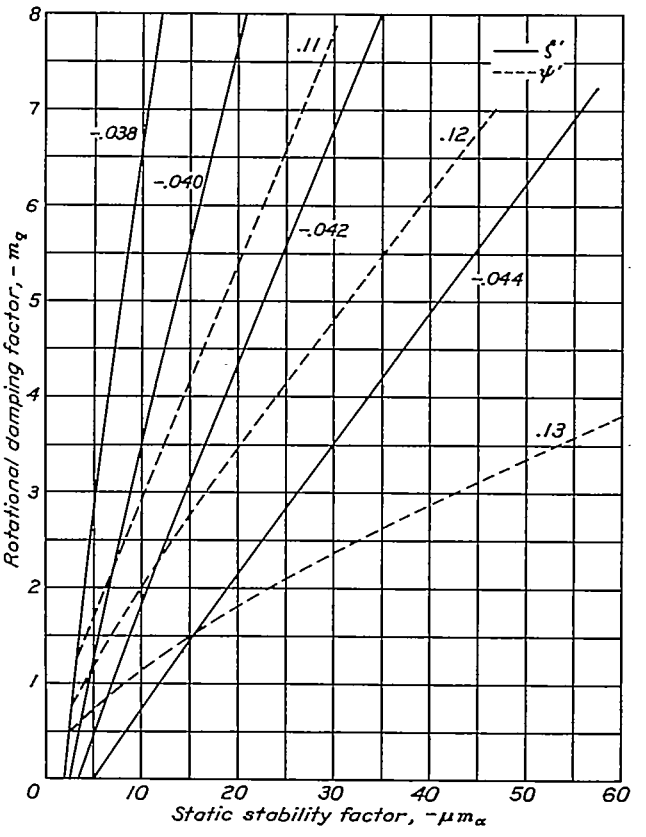

C_L=0.20 C_D=0.064
$\frac{dC_L}{d\alpha}$=4.00 $\frac{dC_D}{d\alpha}$=0.15

FIGURE 20.

FIGURES 15 TO 20.—Dynamic stability charts.

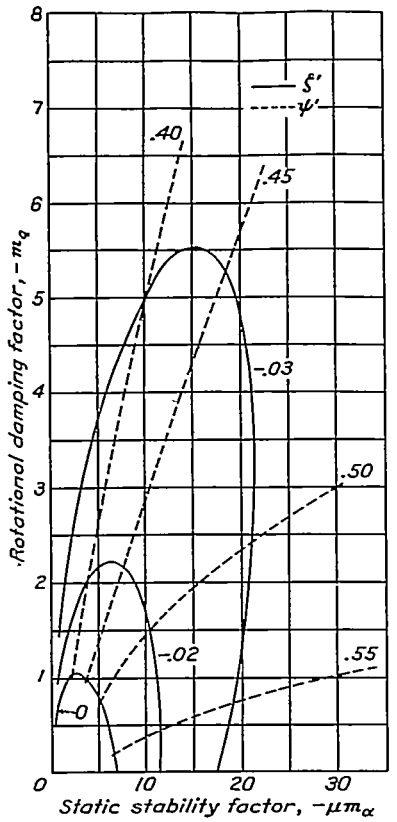

C_L=0.80 C_D=0.065
$\frac{dC_L}{d\alpha}$=4.00 $\frac{dC_D}{d\alpha}$=0.45

FIGURE 21.

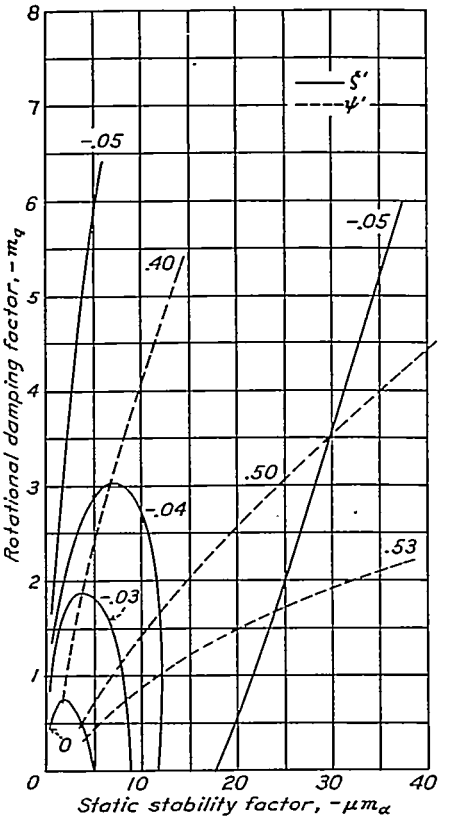

C_L=0.80 C_D=0.091
$\frac{dC_L}{d\alpha}$=4.00 $\frac{dC_D}{d\alpha}$=0.51

FIGURE 23.

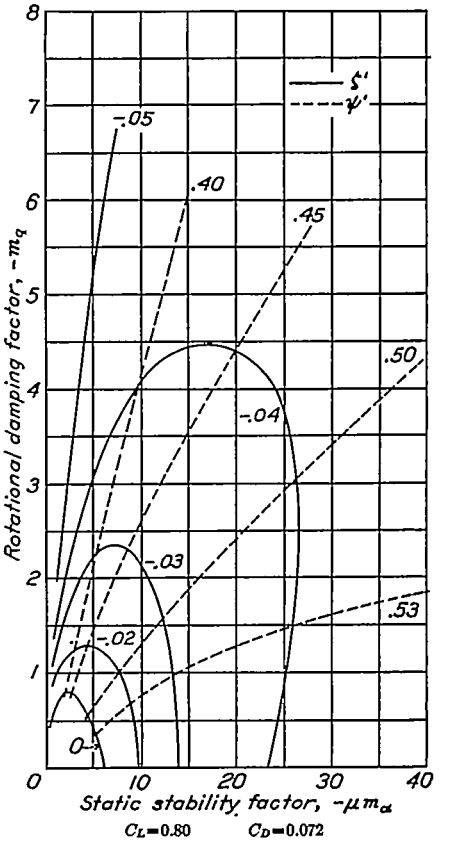

C_L=0.80 C_D=0.072
$\frac{dC_L}{d\alpha}$=4.00 $\frac{dC_D}{d\alpha}$=0.32

FIGURE 25.

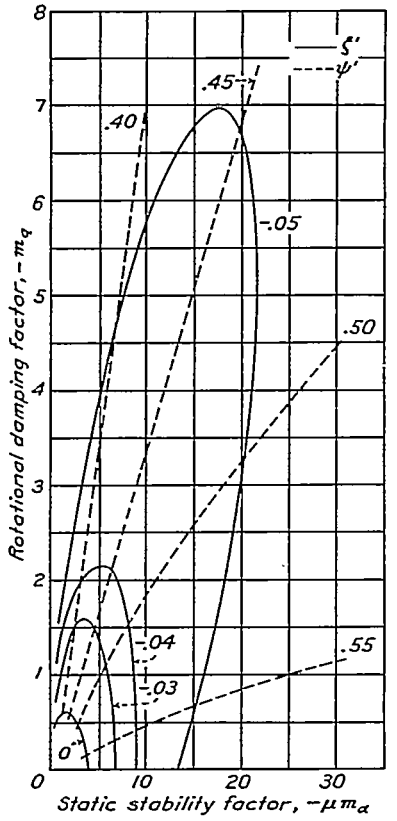

C_L=0.80 C_D=0.091
$\frac{dC_L}{d\alpha}$=3.00 $\frac{dC_D}{d\alpha}$=0.38

FIGURE 22.

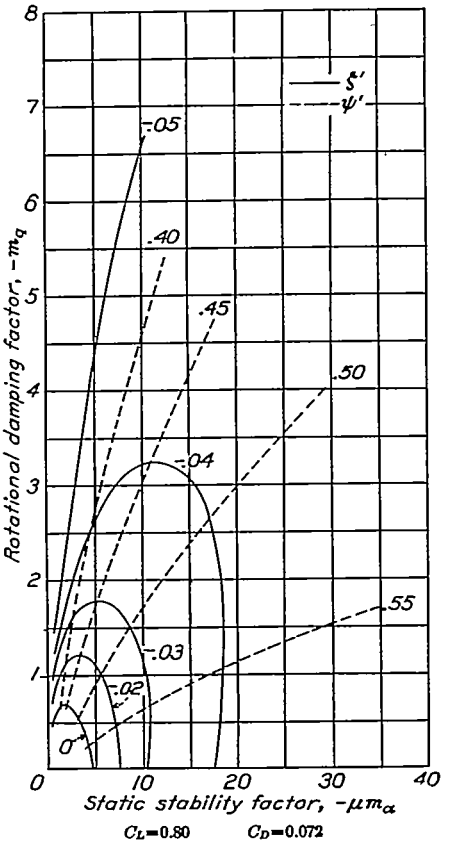

C_L=0.80 C_D=0.072
$\frac{dC_L}{d\alpha}$=3.00 $\frac{dC_D}{d\alpha}$=0.24

FIGURE 24.

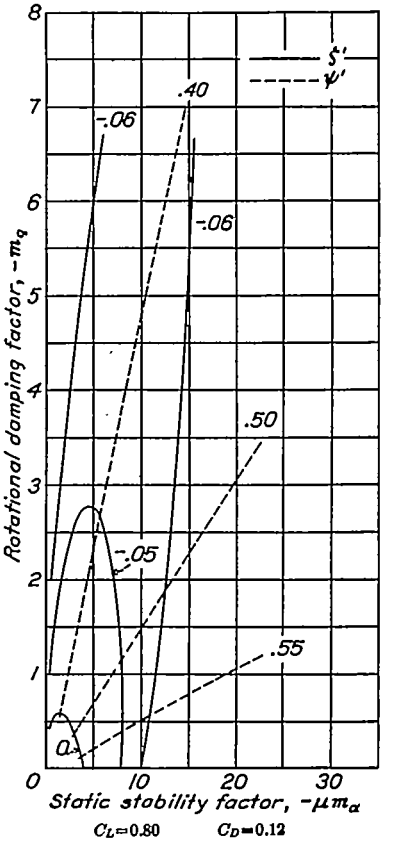

C_L=0.80 C_D=0.12
$\frac{dC_L}{d\alpha}$=4.00 $\frac{dC_D}{d\alpha}$=0.65

FIGURE 26.

FIGURES 21 TO 26.—Dynamic stability charts.

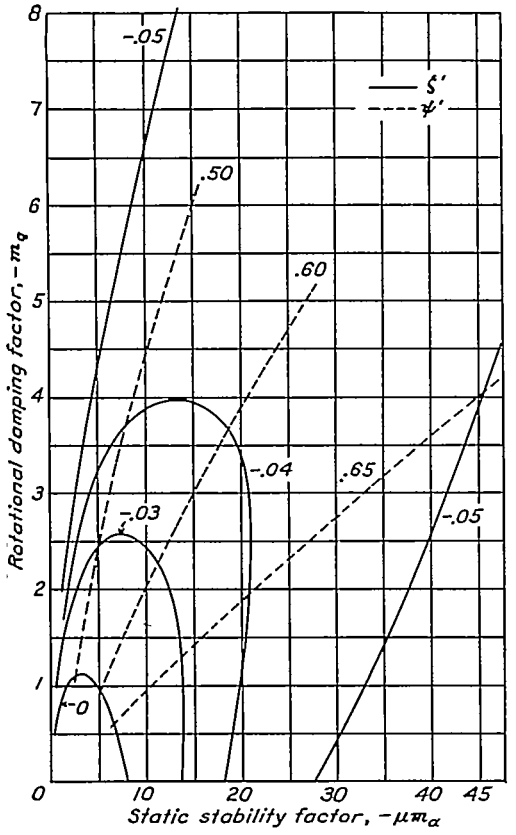

C_L=1.00 C_D=0.091
$\frac{dC_L}{d\alpha}$=4.00 $\frac{dC_D}{d\alpha}$=0.51

FIGURE 27.

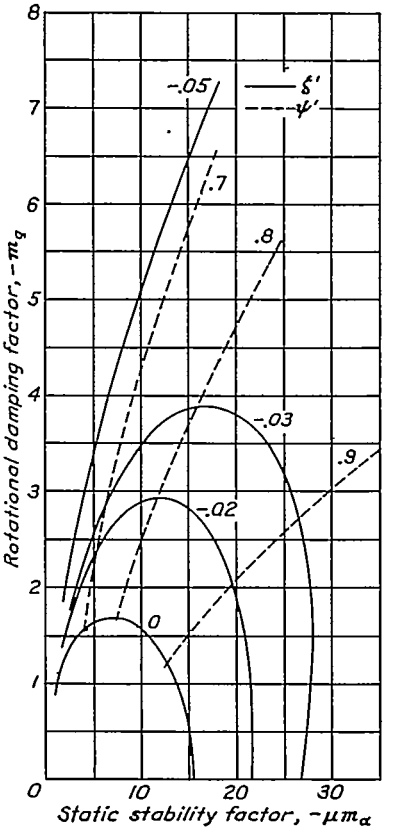

C_L=1.40 C_D=0.091
$\frac{dC_L}{d\alpha}$=4.00 $\frac{dC_D}{d\alpha}$=0.51

FIGURE 29.

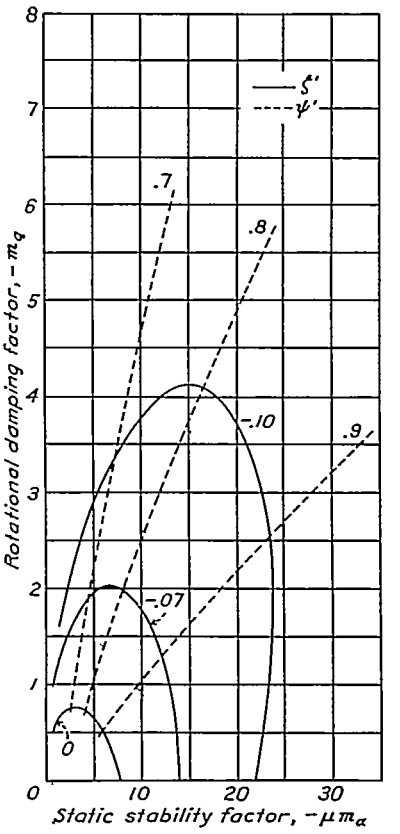

C_L=1.40 C_D=0.20
$\frac{dC_L}{d\alpha}$=4.00 $\frac{dC_D}{d\alpha}$=0.51

FIGURE 31.

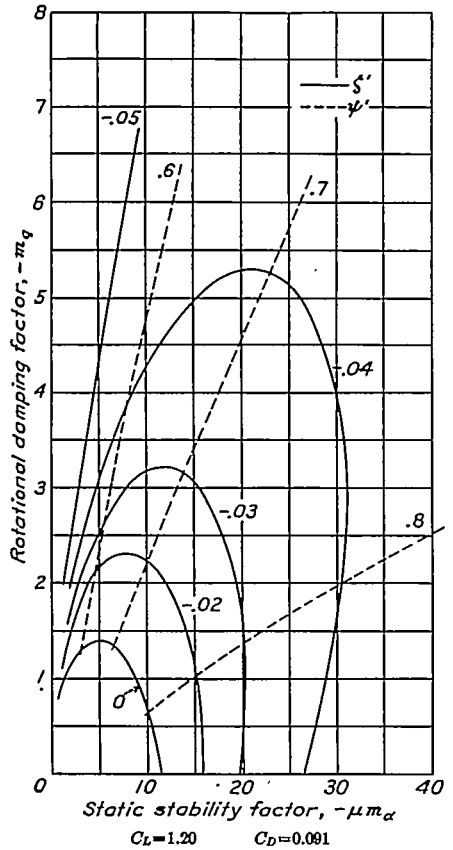

C_L=1.20 C_D=0.091
$\frac{dC_L}{d\alpha}$=4.00 $\frac{dC_D}{d\alpha}$=0.51

FIGURE 28.

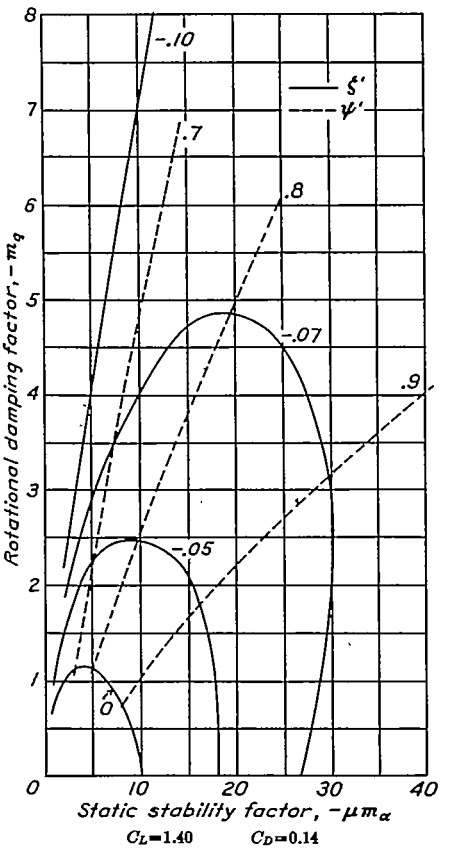

C_L=1.40 C_D=0.14
$\frac{dC_L}{d\alpha}$=4.00 $\frac{dC_D}{d\alpha}$=0.51

FIGURE 30.

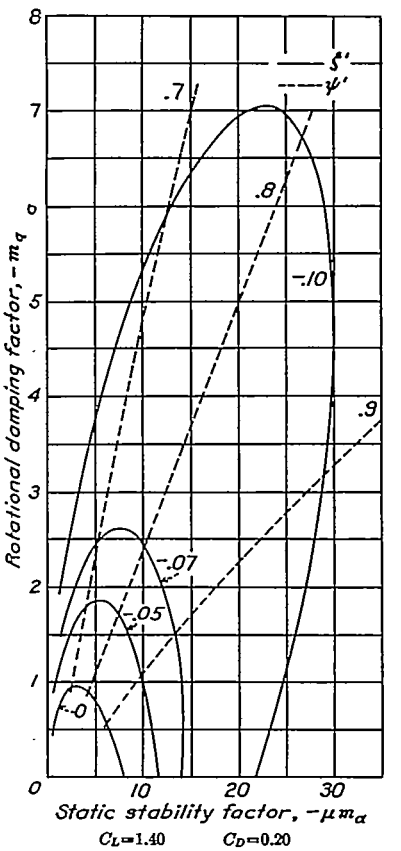

C_L=1.40 C_D=0.20
$\frac{dC_L}{d\alpha}$=4.00 $\frac{dC_D}{d\alpha}$=0.70

FIGURE 32.

FIGURES 27 TO 32.—Dynamic stability charts.

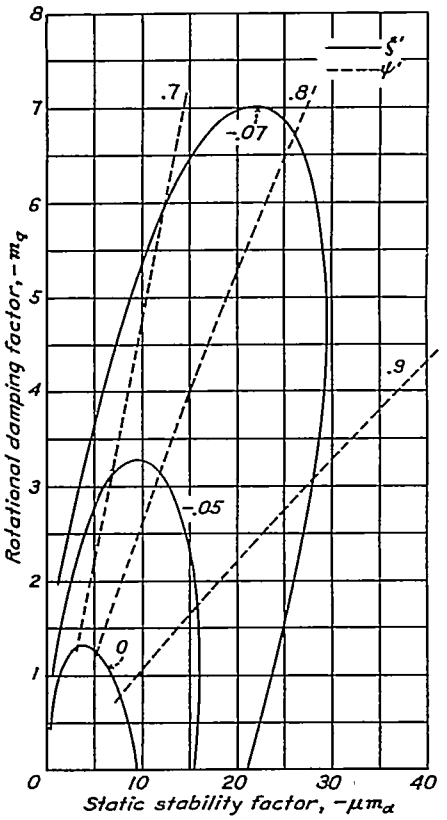

C_L=1.40 C_D=0.16
$\frac{dC_L}{d\alpha}$=4.00 $\frac{dC_D}{d\alpha}$=0.79

FIGURE 33.

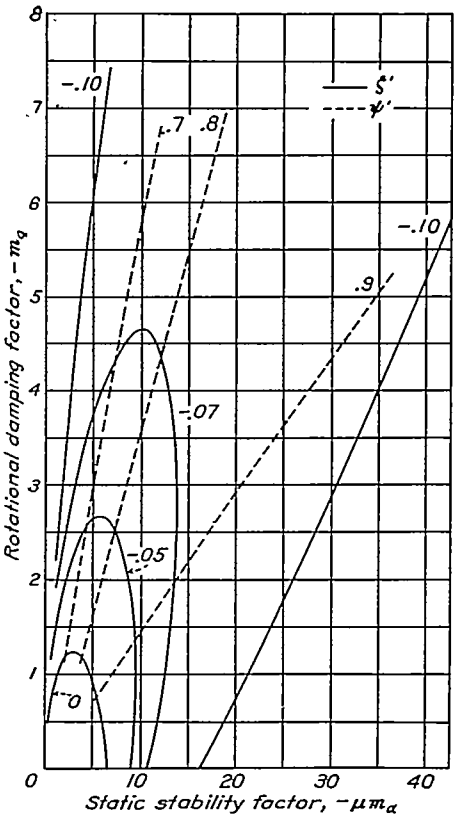

C_L=1.40 C_D=0.20
$\frac{dC_L}{d\alpha}$=3.00 $\frac{dC_D}{d\alpha}$=0.89

FIGURE 35.

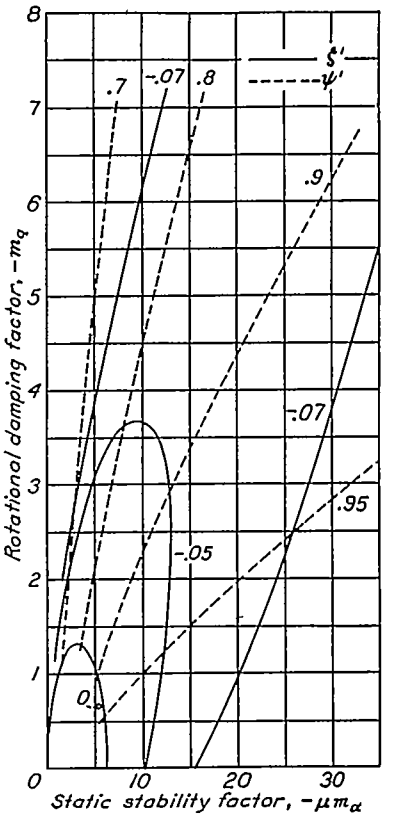

C_L=1.40 C_D=0.14
$\frac{dC_L}{d\alpha}$=2.00 $\frac{dC_D}{d\alpha}$=0.56

FIGURE 37.

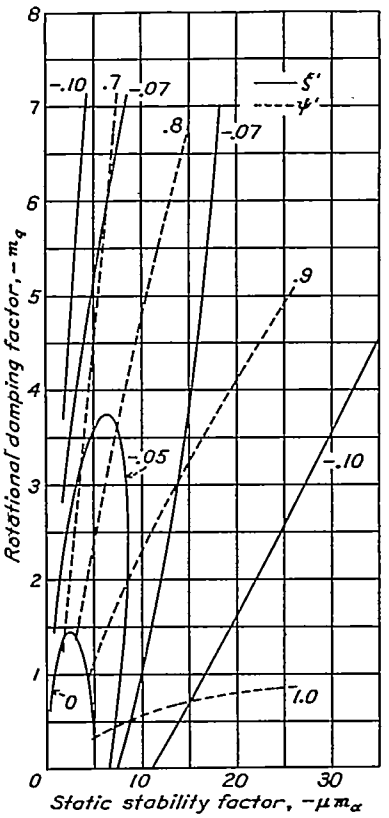

C_L=1.40 C_D=0.20
$\frac{dC_L}{d\alpha}$=2.00 $\frac{dC_D}{d\alpha}$=0.89

FIGURE 34.

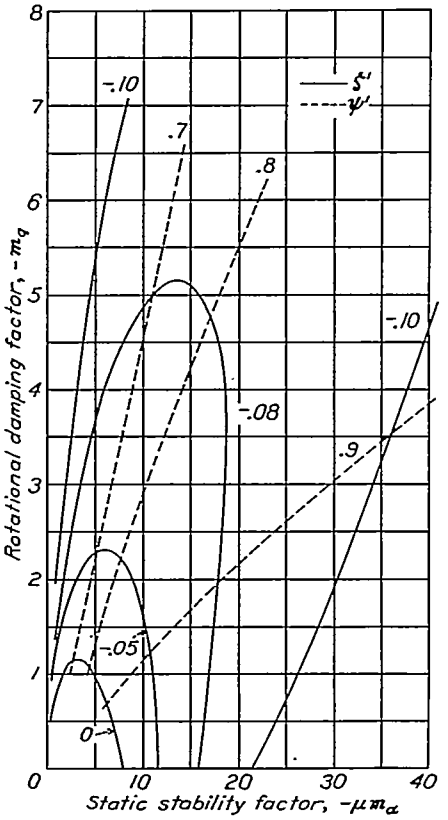

C_L=1.40 C_D=0.20
$\frac{dC_L}{d\alpha}$=4.00 $\frac{dC_D}{d\alpha}$=0.89

FIGURE 36.

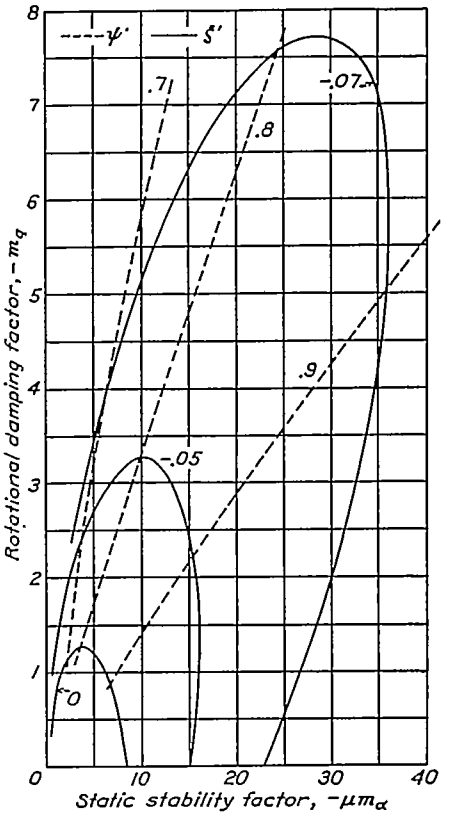

C_L=1.40 C_D=0.14
$\frac{dC_L}{d\alpha}$=3.00 $\frac{dC_D}{d\alpha}$=0.56

FIGURE 38.

FIGURES 33 TO 38.—Dynamic stability charts.

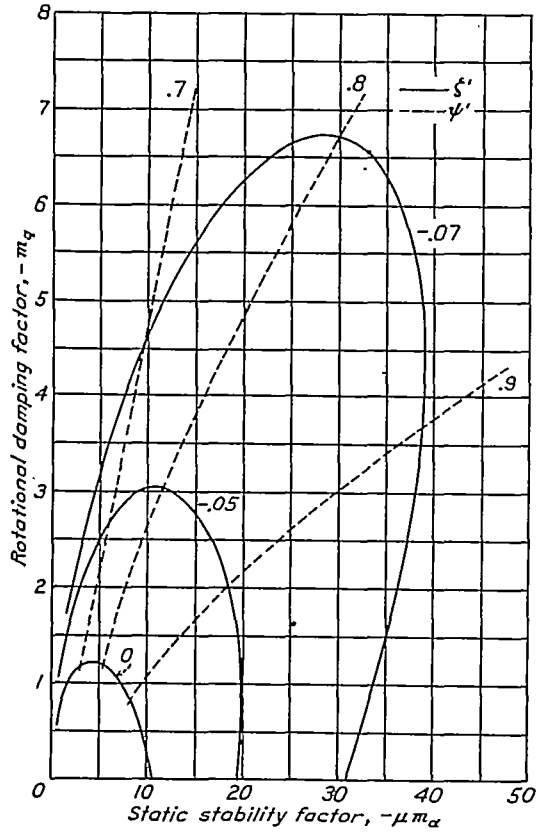

FIGURE 39.

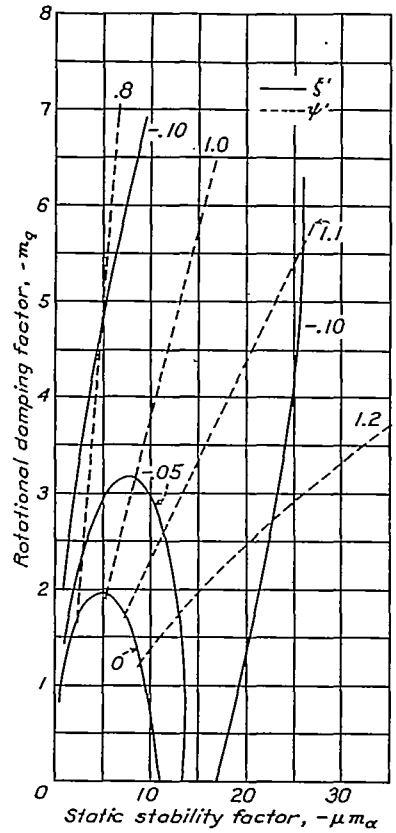

FIGURE 41.

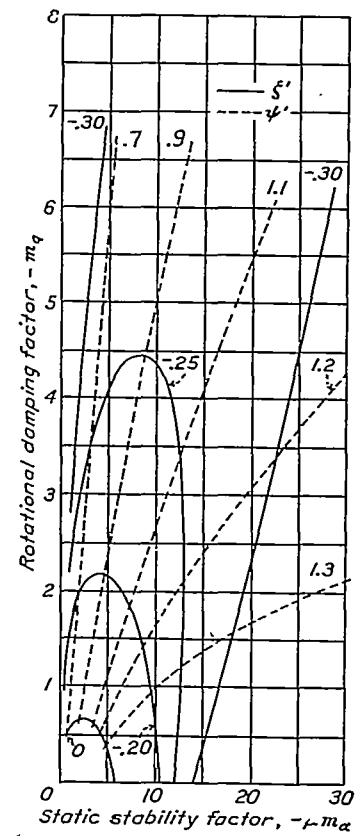

FIGURE 43.

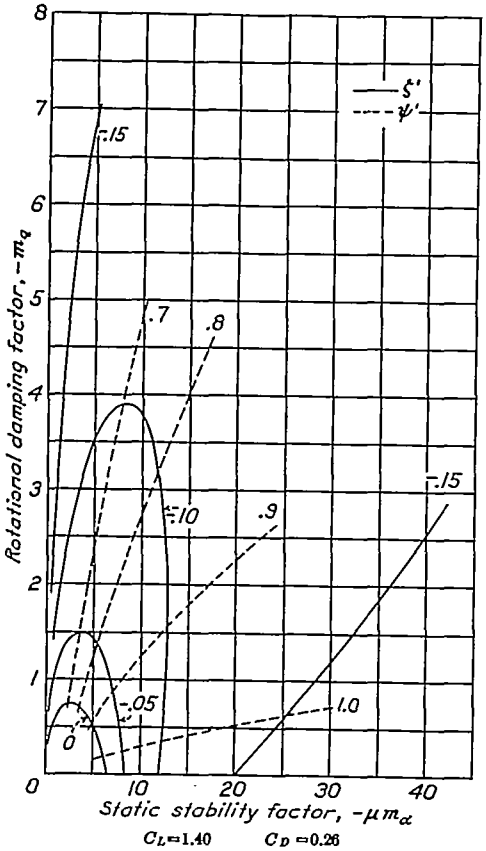

FIGURE 40.

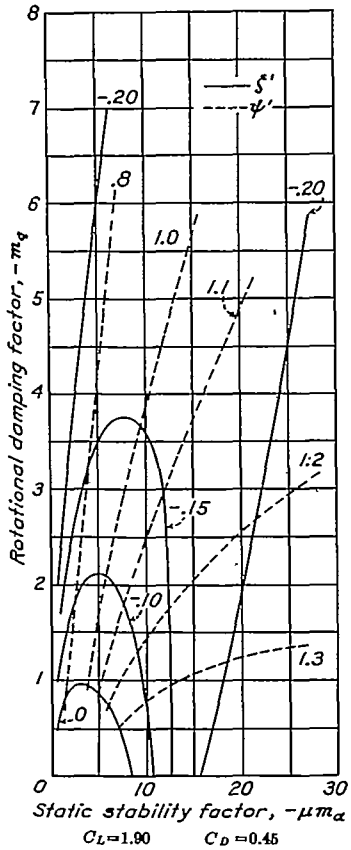

FIGURE 42.

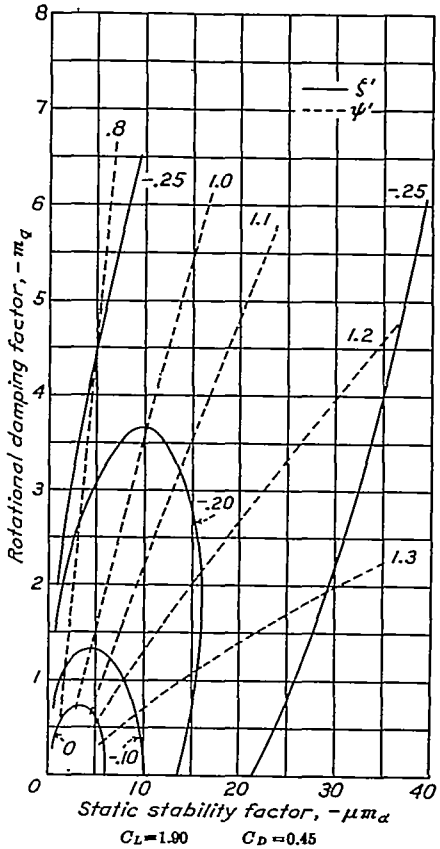

FIGURE 44.

FIGURES 39 TO 44.—Dynamic stability charts.

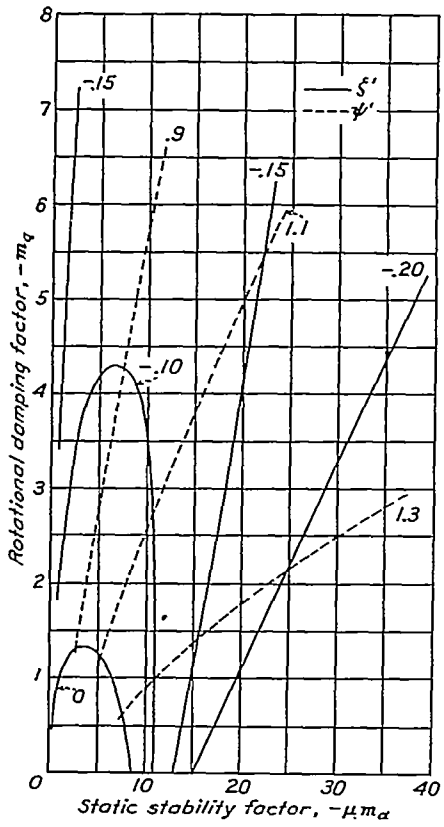

C_L=1.90 C_D=0.45
$\frac{dC_L}{d\alpha}$=4.00 $\frac{dC_D}{d\alpha}$=2.00

FIGURE 45.

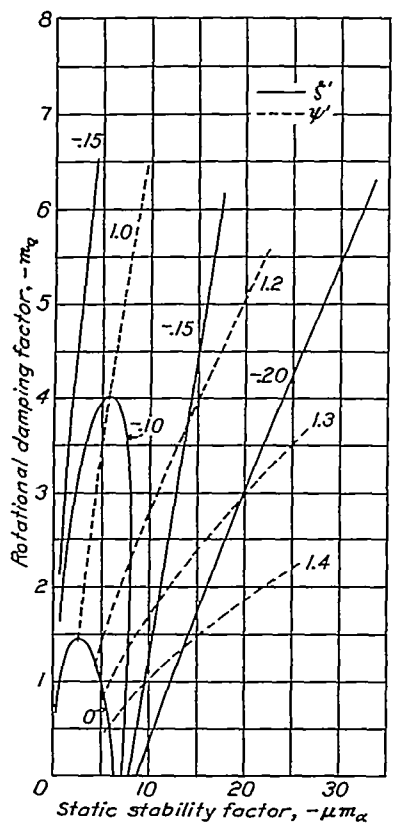

C_L=1.90 C_D=0.45
$\frac{dC_L}{d\alpha}$=2.00 $\frac{dC_D}{d\alpha}$=1.50

FIGURE 47.

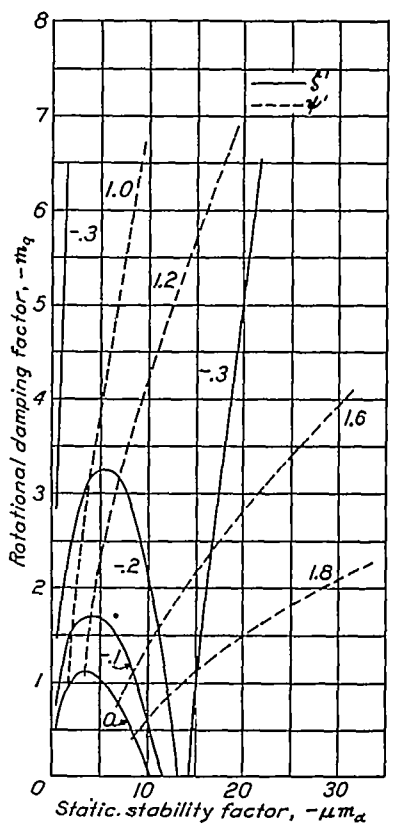

C_L=2.40 C_D=0.85
$\frac{dC_L}{d\alpha}$=4.00 $\frac{dC_D}{d\alpha}$=2.50

FIGURE 49.

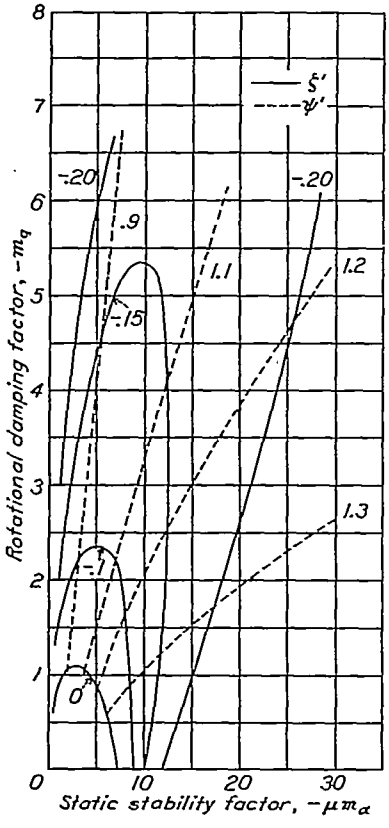

C_L=1.90 C_D=0.45
$\frac{dC_L}{d\alpha}$=3.00 $\frac{dC_D}{d\alpha}$=1.50

FIGURE 46.

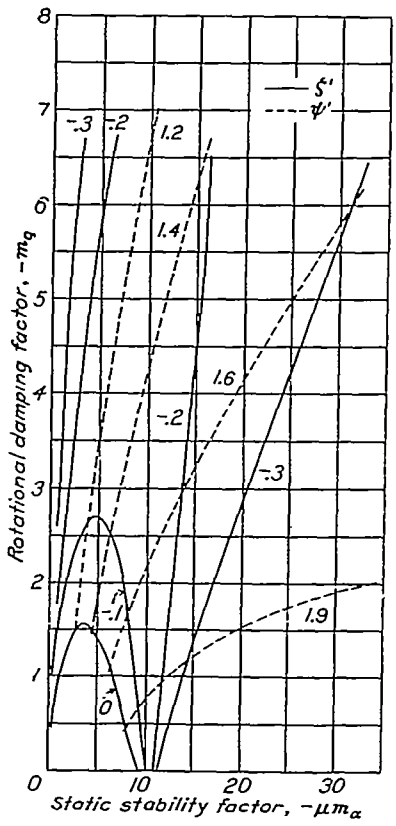

C_L=2.40 C_D=0.70
$\frac{dC_L}{d\alpha}$=4.00 $\frac{dC_D}{d\alpha}$=2.50

FIGURE 48.

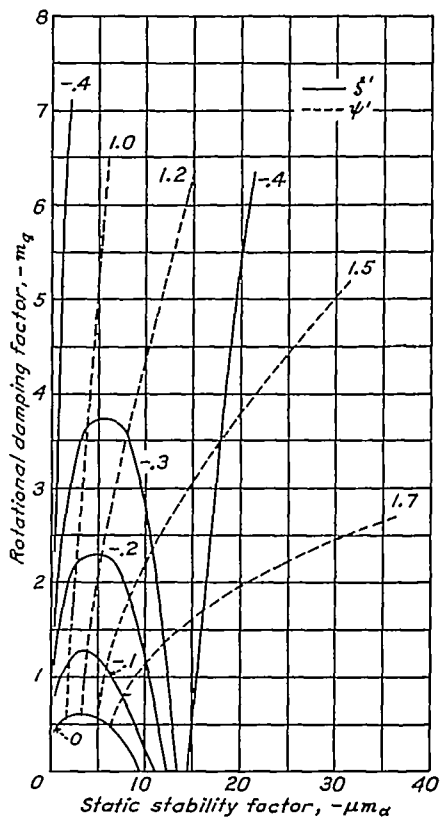

C_L=2.40 C_D=1.00
$\frac{dC_L}{d\alpha}$=4.00 $\frac{dC_D}{d\alpha}$=2.50

FIGURE 50.

FIGURES 45 TO 50.—Dynamic stability charts.

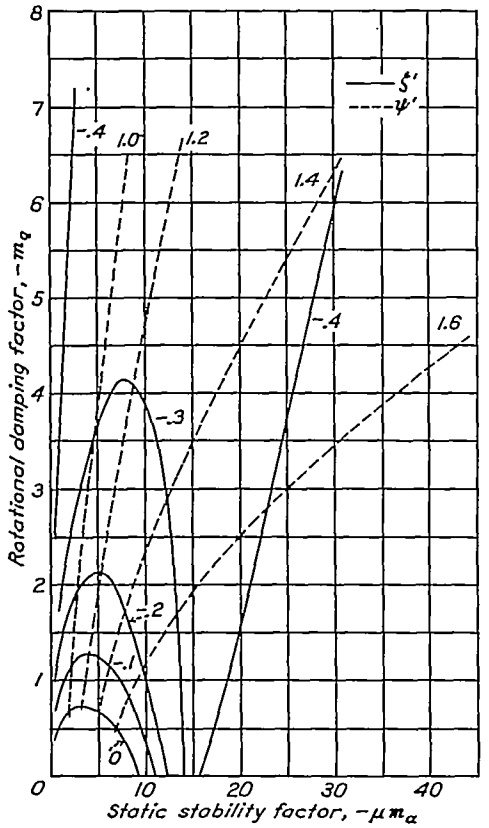

C_L=2.40 C_D=0.85
$\frac{dC_L}{d\alpha}$=4.00 $\frac{dC_D}{d\alpha}$=2.00

FIGURE 51.

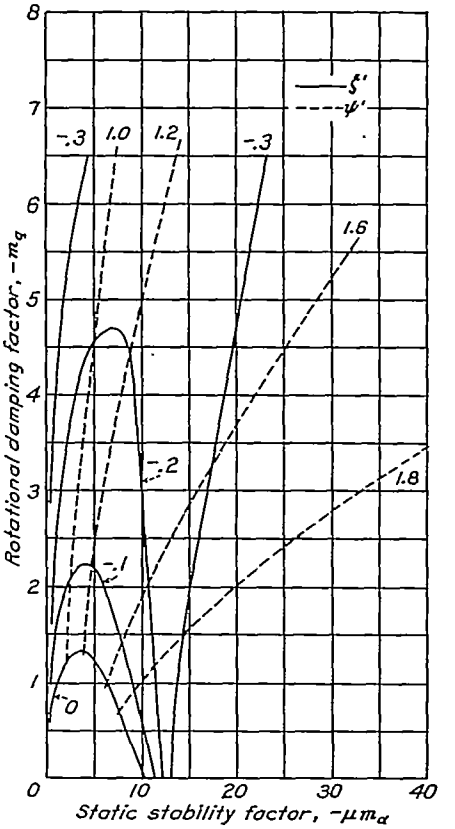

C_L=2.40 C_D=0.85
$\frac{dC_L}{d\alpha}$=3.00 $\frac{dC_D}{d\alpha}$=2.50

FIGURE 53.

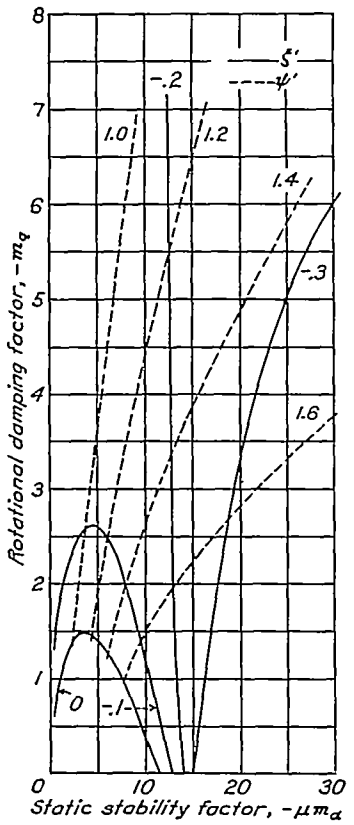

C_L=2.40 C_D=0.85
$\frac{dC_L}{d\alpha}$=4.00 $\frac{dC_D}{d\alpha}$=3.00

FIGURE 52.

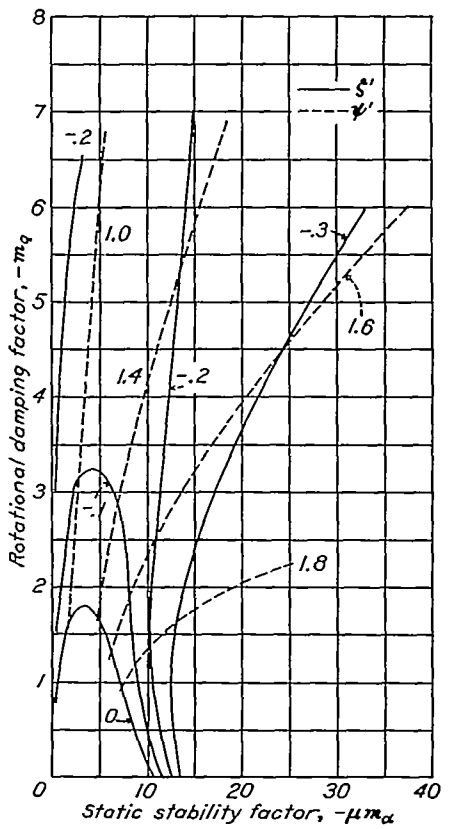

C_L=2.40 C_D=0.85
$\frac{dC_L}{d\alpha}$=2.00 $\frac{dC_D}{d\alpha}$=2.50

FIGURE 54.

FIGURES 51 TO 54.—Dynamic stability charts.

The size of the tail appears in the ratio S_t/S occurring in the expressions for $-m_q$ or $-m_\alpha$. Increasing S_t/S increases both $-m_q$ and $-\mu m_\alpha$. In the case of $-m_q$ the increase is proportional to S_t/S but in the case of $-\mu m_\alpha$ the increase is more than proportional to the increase in S_t/S because $-\mu m_\alpha$ would normally be negative were S_t/S equal to zero. Increasing tail size may be expected to have a net effect somewhat less beneficial than increasing l unless the airplane already has a large value of $-\mu m_\alpha$.

The aspect ratio of the tail surfaces affects the stability through $\frac{dC_{z_t}}{d\alpha_t}$. Increases in $\frac{dC_{z_t}}{d\alpha_t}$ have the same effect as increases in S_t/S and need no further discussion. It will be noticed that if S_t/S is increased by increasing the chord, $\frac{dC_{z_t}}{d\alpha_t}$ will be decreased so that the net effect will be less than would be expected on the basis of tail size alone.

The tail efficiency factor η_t affects the stability characteristics in the same manner as the ratio S_t/S. Tail efficiency depends upon the interference effects of the wings, landing gear, and fuselage upon the tail plane. Warner states (reference 11) that, in general, tail efficiency has been found to range from 0.6 to 0.8 with extreme values as low as 0.54 and as high as 1.2. Computations made by the author for a number of military airplanes indicate that for modern designs the tail efficiency factor will be of the order of 0.75 to 0.8.

The series of charts of stability characteristics against $-m_q$ and $-\mu m_\alpha$ has been extended to include the range of high-lift devices known at the present time (figs. 41 to 54). The charts bear no evidence of increased difficulty with longitudinal stability by the use of these devices. Devices which increase the parasite drag as well as the maximum lift coefficient are more desirable than those which merely serve to maintain the flow to high angles of attack. It will be noticed, however, that in order to use the charts with variable-area lifting surfaces the true area of the extended wing must be used in order to come within the range of parameters given. When the true area is used, S_t/S and μ will have been decreased and the quantity $c(C_q - C_a)$ changed. The effective value of $-m_q$ is thereby decreased as compared with the wing with lifting surfaces contracted; whereas the value of $-\mu m_\alpha$ may be either decreased or increased, depending upon the relative values of the quantities. The fact that an airplane has good stability characteristics with conventional surfaces is therefore no assurance that trouble will not be experienced when high-lift devices, particularly those increasing the wing area, are added. In connection with calculations of stability with high-lift devices it should be noted that in cases of such devices as split flaps, variable-area wings, etc., which greatly increase the camber of the wings, particular attention should be paid to reductions in tail efficiency η_t which may occur in some instances because of the change of effective location of the tail surfaces relative to the wing chord. (See also reference 12.)

The analysis and discussion have been confined to consideration of only the long-period oscillations or the divergence of an airplane as a rigid body. The effects of such physical characteristics as wing or tail-supporting structure elasticity or of free longitudinal controls are not, however, unimportant. No attempt will be made to analyze these effects mathematically but they will be briefly discussed in connection with the basic relationships brought out in the foregoing portions of the report.

The effects of wing elasticity have been treated mathematically in reference 13. Although these effects are normally not important they may in some cases, particularly in view of the high speeds being obtained with modern aircraft, be sufficient to change a normally positive value of $-\mu m_\alpha$ to a negative value with possibly serious tendencies to divergence. The obvious means of guarding against such possibilities are to make the wings rigid in torsion and to use airfoil sections having positive or zero values of C_{m_0}.

The effect of elasticity of the tail-supporting structure is primarily of importance in connection with the phenomena of buffeting and tail flutter and needs no consideration here other than to call attention to the possibility of resonance between the natural frequency of oscillation of the tail structure and the short-period oscillations of the airplane, which are normally very heavily damped. The results of such resonance would probably be structural failure and would not receive practical classification as instability.

The effect of freedom of the longitudinal controls has been treated mathematically in reference 14. The mathematical analysis introduces several new factors into an already complex problem and it seems likely that no designer would attempt to predict the stability with free controls. From a practical standpoint it is obvious that if the control surfaces do not deflect appreciably as the airplane follows the sinusoidal variation of angle of attack, etc., the stability will be the same with free controls as with fixed controls.

The influences that cause the control surfaces to deflect are the aerodynamic hinge moment caused by change of angle of attack of the tail and air speed; the inertia moment that tends to keep the surfaces from following the changes of attitude of the airplane; and the mass moment, in the case of statically unbalanced controls, that tends to deflect the elevator under the influence of gravity and accelerations of the tail plane is accelerated normal to the longitudinal axis. The aerodynamic hinge moment, which is normally of such sign as to decrease $\frac{d\alpha_t}{d\alpha}$ and hence both $-m_q$ and $-\mu m_\alpha$, may be kept small by aerodynamic balance of the elevator surfaces. The inertia moment is small and

may be neglected, as in reference 14. The mass moment may be kept small by statically balancing the elevator.

It follows from the foregoing discussion that stability with free controls can be insured by providing ample stability with fixed controls and then aerodynamically and statically balancing the elevator surfaces or making the control irreversible. It is generally not desirable to attain complete aerodynamic balance, but the difference between the stability with free controls and that with fixed controls can be made small without complete aerodynamic balance or without making the controls completely irreversible.

CONCLUSIONS

1. It is believed that for the average student of the subject this substitute treatment of the derivation of the relationships governing longitudinal stability will be more understandable than the classical treatment.

2. Increase in the amplitude of longitudinal oscillations with time is possible only when the change in angle of attack lags the change in flight-path angle. The lag of the angle of attack with respect to the flight-path angle depends primarily upon the static-stability factor $-\mu m_\alpha$.

3. The nondimensional parameter $-\mu m_\alpha$ not only plays the most important part in determining the lag of the angle of attack with respect to the flight-path angle but also is the only source of unstabilizing angular momentum with power off. Increasing the value of $-\mu m_\alpha$, i. e., increasing the static stability, will increase the tendency to instability if the original value of $-\mu m_\alpha$ is small. After a certain value of $-\mu m_\alpha$ is reached, further increases in the negative sense will reduce the tendency to instability.

4. The effect of the vertical location of the wing relative to the center of gravity should not be neglected in calculating the static stability.

5. Aerodynamically efficient airplanes are more likely to be dynamically unstable than less efficient types.

6. Increasing the wing loading will increase the period of the oscillations but will not necessarily make the airplane either more or less stable.

7. High-lift devices that depend partly upon increases in wing area may lead to instability if the size and disposition of the tail surfaces are determined on the basis of the contracted wing.

8. There is no likelihood of dynamic instability at the angle of attack corresponding to maximum or cruising speeds. The damping of the oscillations may be more or less pronounced at low speeds than at high speeds. There is likelihood of dynamic instability at low speeds.

9. Stability with free controls can be brought close to that with fixed controls by aerodynamically and statically balancing the elevators.

II. ESTIMATION OF STABILITY

METHOD

The charts included in this report (figs. 15 to 54) provide an easy method of estimating the dynamic stability of airplanes. In order to use the charts it is necessary to know the values of the nondimensional parameters C_L, C_D, $\frac{dC_L}{d\alpha}$, $\frac{dC_D}{d\alpha}$, $-m_q$, and $-\mu m_\alpha$ for the airplane at the speed under consideration. Knowing the parameters, turn to the charts and select those for which C_L, C_D, $\frac{dC_L}{d\alpha}$ and $\frac{dC_D}{d\alpha}$ most nearly represent the case under consideration. Spot the particular point representing $-m_q$ and $-\mu m_\alpha$ upon the charts. Rough interpolations between the values of ζ' and ψ' so indicated will, in general, provide a sufficiently accurate estimation of the stability characteristics of the design. The time to damp to one-half amplitude, in seconds, is

$$T=\frac{-0.313\sqrt{\frac{W}{S}C_L}}{\zeta'}$$

and the period in seconds is

$$P=\frac{2.83\sqrt{\frac{W}{S}C_L}}{\psi'}$$

The number of oscillations for the amplitude to die to one-half the original value will be $\frac{T}{P}=-\frac{\psi'}{9\zeta'}$.

DETERMINATION OF NONDIMENSIONAL PARAMETERS

The nondimensional parameters should be taken from available flight or wind-tunnel data if possible. If such data cannot be obtained they may be calculated by methods outlined in the following paragraphs.

Lift coefficient C_L.—The lift coefficient C_L follows directly from the wing loading and the speed. In general, it is desirable to choose C_L as 0.20, 0.80, 1.40, 1.90, or 2.40 to facilitate use of the charts. For airplanes with variable-area wings the wing area in use under the flight condition should be used as the basis of calculations.

Drag coefficient C_D.—The drag coefficient C_D may be estimated from the relationship

$$C_D=C_{D_p}+\frac{C_L^2}{\pi\frac{(kb)^2}{S}e}\quad\text{(see reference 6)}$$

where C_{D_p} is the parasite-drag coefficient,

$\frac{(kb)^2}{S}$, the equivalent monoplane aspect ratio (reference 7 gives k in convenient form).

e, an airplane efficiency factor ranging from 1 for very clean designs to 0.7 for very inefficient designs (reference 6).

Slope of lift curve $\frac{dC_L}{d\alpha}$.—The slope of the lift curve $\frac{dC_L}{d\alpha}$ may be taken as 4 (all values of angles are in radian measure) at low and intermediate angles of attack and as 3 near the stall if the values of the other parameters are based on the true wing area and the airplane is a conventional type. It should be noted that in cases of extremely high or extremely low aspect ratios for which $\frac{dC_L}{d\alpha}$ differs considerably from 4 the wing area may be considered such as to make $\frac{dC_L}{d\alpha}=4$ if C_L, C_D, and $\frac{dC_D}{d\alpha}$, $-m_q$, μ, and $-m_\alpha$ are each multiplied by the ratio of 4 to the actual value of $\frac{dC_L}{d\alpha}$ for reference to the charts. In such a case the ratio must not be neglected in the conversion to time in seconds.

Slope of the drag curve $\frac{dC_D}{d\alpha}$.—The slope of the drag curve may be estimated from the relationship

$$\frac{dC_D}{d\alpha}=\frac{2C_L\frac{dC_L}{d\alpha}}{\pi\frac{(kb)^2}{S}e}$$

The value of $\frac{dC_L}{d\alpha}$ here used may be taken as 4 throughout the flight range as $\frac{dC_D}{d\alpha}$ does not fall off with $\frac{dC_L}{d\alpha}$ near the stall.

Rotational damping factor $-m_q$.—This parameter will, in general, have to be estimated although it may be determined from tests of an oscillating model, or from tests on a whirling arm (reference 15). For purposes of estimation the equation

$$-m_q=K\eta_t\frac{l^2}{2k_Y^2}\frac{S_t}{S}\frac{dC_{L_t}}{d\alpha_t}$$

where K is taken as 1.25 will generally be sufficiently accurate. The tail efficiency η_t may be taken as 0.75 or 0.80 for modern designs. The distance from the center of gravity to the elevator quarter-chord point l, the ratio of tail-plane area to wing area S_t/S, and the radius of gyration of the airplane about the span axis k_Y are dimensional characteristics of the airplane. The radius of gyration may be found from the relationship

$$k_Y=\sqrt{\frac{B}{W}g}$$

where

B is the moment of inertia about the span axis.

g, the acceleration of gravity.

W, weight of the airplane.

or estimated from the relationship

$$k_Y=\sqrt{C_B(l_1^2+h^2)}$$

where

C_B is an empirical constant.

l_1, over-all length of the airplane.

h, over-all height of the airplane.

From 11 airplanes for which C_B was determined (reference 16)

$0.0325\leqq C_B\leqq 0.0394$ with the average value 0.0362.

In the absence of test data the slope of the lift curve for the tail may be taken as

$$\frac{dC_{L_t}}{d\alpha_t}=\frac{5.5}{1+\frac{2}{\frac{b_t^2}{S_t}}}\text{ (reference 17)}$$

Static stability factor $-\mu m_\alpha$.—The static stability factor is

$$-\mu m_\alpha=-\frac{W}{S\rho\times 32.2\times l}\frac{lc}{2k_Y^2}\frac{dC_{m_{c.g.}}}{d\alpha}$$

or

$$-\frac{6.5\frac{W}{S}c}{k_Y^2}\frac{dC_{m_{c.g.}}}{d\alpha}\text{ (standard conditions)}$$

where c is the chord length upon which C_m is based. Various methods have been proposed for estimating $\frac{dC_{m_{c.g.}}}{d\alpha}$. The author prefers the relationship

$$\frac{dC_{m_{c.g.}}}{d\alpha}=\frac{dC_L}{d\alpha}(C_g-C_a)+\frac{dC_{X_w}}{d\alpha}\frac{z}{c}+\frac{dC_{m_p}}{d\alpha}-\eta_t\frac{l}{c}\frac{S_t}{S}\frac{dC_{L_t}}{d\alpha_t}\frac{d\alpha_t}{d\alpha}$$

where

C_g is the distance of the center of gravity of the airplane from the leading edge of the reference chord in chord lengths.

C_a, the distance of the aerodynamic center of the wings (reference 8) from the leading edge of the reference chord in chord lengths.

$\frac{dC_{X_w}}{d\alpha}$, the slope of the curve of longitudinal force coefficient for the wings alone against angle of attack and is

$$\frac{dC_{X_w}}{d\alpha}=\left(C_L-\frac{dC_{D_w}}{d\alpha}\right)\cos\alpha+\left(C_{D_w}+\frac{dC_L}{d\alpha}\right)\sin\alpha$$

where $\frac{dC_{D_w}}{d\alpha}$ and C_{D_w} are values for the wing alone.

$\frac{z}{c}$, the distance of the reference chord below the center of gravity in chord lengths.

$\frac{dC_{m_p}}{d\alpha}$, the slope of parasite pitching moment due to fuselage, engine nacelles, landing gear, etc., against angle of attack.

$\frac{d\alpha_t}{d\alpha}$, the rate of change of the angle of attack at the tail with change of angle of attack of the airplane and is

$\frac{d\alpha_t}{d\alpha}=1-\frac{d\epsilon}{d\alpha}$ where ϵ is the angle of downwash at the tail.

The value of C_a varies from 0.23 to 0.25 referred to the mean aerodynamic chord of conventional airfoils (reference 9). The value of $\frac{dC_{m_p}}{d\alpha}$ may be estimated if the designer so desires. The author has found the value to vary from 0 to 0.4 for a few military airplanes at low angles of attack with the average value about 0.2. The value of $\frac{dC_{m_p}}{d\alpha}$ was found, for the cases considered, to fall off to approximately zero at high angles of attack.

The rate of change of downwash angle at the tail with change of angle of attack may be estimated from the relationship

$$\frac{d\epsilon}{d\alpha}=\frac{1.05}{\frac{(kb)^2}{S}}(x+1)^{-0.38}(y+1)^{-0.23}\frac{dC_L}{d\alpha} \text{ (reference 10)}$$

where

$\frac{dC_L}{d\alpha}$ is in radian measure

x, the distance of the tail plane to the rear of the trailing edge of the wing in chord lengths.

y, the distance of the tail plane above or below the trailing edge of the wing in chord lengths.

For the average case $y=0$, $x=2.5$, $\frac{d\epsilon}{d\alpha}=\frac{0.65}{\frac{(kb)^2}{S}}\frac{dC_L}{d\alpha}$

EXAMPLES

AIRPLANE A

$C_L=0.80$ $\qquad \frac{dC_L}{d\alpha}=3.95$

$C_D=0.080$ $\qquad \frac{dC_D}{d\alpha}=0.39$

(Taken from full-scale flight data.)

$-m_q=2.6$ $\qquad -\mu m_\alpha=16.5$

(Estimated.)

From figure 23 $\zeta'=-0.044$ $\psi'=0.48$

From figure 25 $\zeta'=-0.035$ $\psi'=0.48$

From interpolation between the figures on the basis of C_D, $\zeta'=-0.039$ and $\psi'=0.48$. From interpolation between the figures on the basis of $\frac{dC_D}{d\alpha}$, $\zeta'=-0.038$ and $\psi'=0.48$. From full-scale unpublished flight tests of this airplane $\zeta'=-0.041$ and $\psi'=0.72$.

AIRPLANE B

$C_L=0.80$ $\qquad \frac{dC_L}{d\alpha}=3.60$

$C_D=0.076$ $\qquad \frac{dC_D}{d\alpha}=0.42$

$-m_q=1.5$ $\qquad -\mu m_\alpha=9$

(Taken from full-scale flight data.)

From figure 23 $\zeta'=-0.034$ $\psi'=0.49$

From figure 24 $\zeta'=-0.030$ $\psi'=0.50$

From figure 25 $\zeta'=-0.025$ $\psi'=0.48$

From interpolation between figures 23 and 24 on the basis of C_D, $\zeta'=-0.031$ and $\psi'=0.50$. From interpolation between figures 23 and 24 on the basis of $\frac{dC_D}{d\alpha}$, $\zeta'=-0.033$ and $\psi'=0.49$. From interpolation between figures 24 and 25 on the basis of $\frac{dC_L}{d\alpha}$, $\zeta'=-0.027$ and $\psi'=0.49$.

From full-scale flight tests of this airplane (reference 2) $\zeta'=-0.038$ and $\psi'=0.55$.

AIRPLANE C

$C_L=0.80$ $\qquad \frac{dC_L}{d\alpha}=4.00$

$C_D=0.094$ $\qquad \frac{dC_D}{d\alpha}=0.51$

$-m_q=2.3$ $\qquad -\mu m_\alpha=4.8$

(Estimated data.)

From figure 23, $\zeta'=-0.034$ and $\psi'=0.4$.

No interpolation is necessary. From extrapolation of full-scale unpublished flight data $\zeta'=-0.030$ and $\psi'=0.72$.

AIRPLANE D

$C_L=0.80$ $\qquad \frac{dC_L}{d\alpha}=4.00$

$C_D=0.12$ $\qquad \frac{dC_D}{d\alpha}=0.54$

$-m_q=1.76$ $\qquad -\mu m_\alpha=3.40$

(Estimated data.)

From figure 26, $\zeta'=-0.03$ to -0.04 and $\psi'=0.39$.

From full-scale unpublished data $\zeta'=-0.035$ and $\psi'=0.53$.

LANGLEY MEMORIAL AERONAUTICAL LABORATORY,
NATIONAL ADVISORY COMMITTEE FOR AERONAUTICS,
LANGLEY FIELD, VA., *December 13, 1934*

APPENDIX

RECAPITULATION OF SYMBOLS

A, B, C, D, E, coefficients of stability quartic.

a, b, coefficients of stability quadratic.

$c=\frac{1}{2}\left(3C_D+\frac{dC_L}{d\alpha}\right)$

$d=\frac{1}{2}\left(C_D\frac{dC_L}{d\alpha}-C_L\frac{dC_D}{d\alpha}+C_R^2\right)$

$e=\frac{3}{2}C_D$

$f=\frac{1}{2}C_R^2$

e, base of natural logarithms.

e, airplane efficiency factor such that $C_{D_t}=\frac{C_L^2}{e\pi\frac{(kb)^2}{S}}$

C_R, coefficient of resultant force.

C_Z, coefficient of force normal to the wing chord, positive downward.

C_X, coefficient of force parallel to the wing chord, positive forward.

C_a, coefficient of aerodynamic center (ratio of distance of aerodynamic center from leading edge to chord length).

C_g, coefficient of center of gravity (ratio of distance of center of gravity from leading edge to chord length).

C_{m_p}, coefficient of pitching moment other than that from wings and horizontal tail surfaces.

C_{m_0}, coefficient of pitching moment of wing at zero lift.

$C_{m_{c.g.}}$, coefficient of pitching moment with respect to center of gravity.

$C_B=\frac{k_Y^2}{(l_1^2+h^2)}$, coefficient of radius of gyration about lateral axis.

l_1, over-all length of airplane.

h, over-all height of airplane.

l, distance from center of gravity to quarter-chord point of horizontal tail surfaces.

$i=\sqrt{-1}$

K, empirical factor by which computed value of rotational damping factor of tail is multiplied to give total rotational damping factor.

k, empirical factor for conversion of biplane span to equivalent monoplane span.

$-\mu m_\alpha=-\frac{m}{\rho Sl}\frac{lc}{2k_Y^2}\frac{dC_{m_{c.g.}}}{d\alpha}$, static-stability factor.

$-m_q=K\eta_t\frac{l^2}{2k_Y^2}\frac{S_t}{S}\frac{dC_{L_t}}{d\alpha_t}$, rotational damping factor.

0, subscript denoting that the value of the symbol refers to zero time.

P', period of an oscillation, nondimensional units.

P, period of an oscillation, seconds.

T', time for an oscillation to decrease to one-half amplitude, nondimensional units.

T, time for an oscillation to decrease to one-half amplitude, seconds.

t, subscript denoting that the symbol refers to the horizontal tail surfaces.

$\Delta V'$, ratio of ΔV to V.

w, subscript denoting that the symbol refers to the wing alone.

x, distance of horizontal tail surfaces to the rear of the trailing edge of the wing, chord lengths.

y, distance of horizontal tail surfaces above or below the wing chord (extended), chord lengths.

z, distance of wing chord below center of gravity.

δ_1, angle of lag of change in angle of attack with respect to change in angle of flight path.

δ_2, angle of lag of change in velocity along flight path with respect to change in angle of flight path.

δ_3, angle of lag of change in angle of pitch with respect to change in angle of flight path.

δ_4, angle of lag of change of angle of attack with respect to change in angle of pitch.

η_t, tail efficiency.

$\zeta'=-\frac{0.693}{T'}$, damping coefficient.

$\psi'=\frac{2\pi}{P'}$, period coefficient.

$\lambda'=\zeta'\pm i\psi'$.

$\mu=\frac{m}{\rho Sl}$, relative density.

$\tau=\frac{m}{\rho SV}$, time conversion factor.

REFERENCES

1. Bairstow, L., Jones, B. Melvill, and Thompson, A. W. H.: Investigation into the Stability of an Aeroplane, with an Examination into the Conditions Necessary in Order that the Symmetric and Asymmetric Oscillations Can Be Considered Independently. R. & M. No. 77, British A. C. A., 1913.
2. Soulé, Hartley A., and Wheatley, John B.: A Comparison between the Theoretical and Measured Longitudinal Stability Characteristics of an Airplane. T. R. No. 442, N. A. C. A., 1932.

3. Glauert, H.: A Non-Dimensional Form of the Stability Equations of an Aeroplane. R. & M. No. 1093, British A. R. C., 1927.
4. Routh, E. J.: Advanced Rigid Dynamics, vol. II. The MacMillan Company, 1905.
5. Gates, S. B.: A Survey of Longitudinal Stability below the Stall, with an Abstract for Designers' Use. R. & M. No. 1118, British A. R. C., 1928.
6. Oswald, W. Bailey: General Formulas and Charts for the Calculation of Airplane Performance. T. R. No. 408, N. A. C. A., 1932.
7. Diehl, Walter S.: Two Practical Methods for the Calculation of the Horizontal Tail Area Necessary for a Statically Stable Airplane. T. R. No. 293, N. A. C. A., 1928.
8. Munk, Max M.: Elements of the Wing Section Theory and of the Wing Theory. T. R. No. 191, N. A. C. A., 1924.
9. Jacobs, Eastman N., Ward, Kenneth E., and Pinkerton, Robert M.: The Characteristics of 78 Related Airfoil Sections from Tests in the Variable-Density Wind Tunnel. T. R. No. 460, N. A. C. A., 1933.
10. Reid, Elliott G.: Applied Wing Theory. McGraw-Hill Book Company, Inc., 1932, p. 196.
11. Warner, Edward P.: Airplane Design. Aerodynamics. McGraw-Hill Book Company, Inc., 1927, p. 343.
12. Hirst, D. M., and Hartshorn, A. S.: The Efficiency of a Tail Plane behind a Wing of R. A. F. 34 Section. R. & M. No. 1478, British A. R. C., 1932.
13. Pugsley, A. G.: Influence of Wing Elasticity upon the Longitudinal Stability of an Aeroplane. R. & M. No. 1548, British A. R. C., 1933.
14. Glauert, H.: The Longitudinal Stability of an Aeroplane. R. & M. No. 638, British A. C. A., 1919.
15. Halliday, A. S., Bryant, L. W., and Burge, C. H.: The Experimental Determination of Pitching Moment of an Aeroplane Due to Rotation in Pitch. R. & M. No. 1556, British A. R. C., 1933.
16. Miller, Marvel P., and Soulé, Hartley A.: Moments of Inertia of Several Airplanes. T. N. No. 375, N. A. C. A., 1931.
17. Higgins, George J.: The Prediction of Airfoil Characteristics. T. R. No. 312, N. A. C. A., 1929.

BIBLIOGRAPHY

Bairstow, Leonard: Applied Aerodynamics. Longmans, Green and Co., 1920.
Bryan, G. H.: Stability in Aviation. MacMillan and Co., Ltd., London, 1911.
Haus, Fr.: Automatic Stability of Airplanes. T. M. No. 695, N. A. C. A., 1932.
Lanchester, F. W.: Aerodonetics. Constable & Co., Ltd., London, 1917.
Wilson, Edwin Bidwell: Aeronautics. John Wiley and Sons, Inc., 1920.

TABLE I

LIST OF CHARTS

Figure	C_L	$\frac{kb^2}{S}$	C_{D_p}	C_D	$\frac{dC_L}{d\alpha}$	$\frac{dC_D}{d\alpha}$
15	0.20	5	0.02	0.023	4.00	0.11
16	.20	5	.04	.043	3.00	.10
17	.20	5	.04	.043	4.00	.13
18	.20	8	.04	.042	3.00	.06
19	.20	8	.04	.042	4.00	.08
20	.20	5	.06	.064	4.00	.15
21	.80	5	.02	.065	4.00	.45
22	.80	5	.04	.091	3.00	.33
23	.80	5	.04	.091	4.00	.51
24	.80	8	.04	.072	3.00	.24
25	.80	8	.04	.072	4.00	.32
26	.80	5	.06	.120	4.00	.65
27	1.00			.091	4.00	.51
28	1.20			.091	4.00	.51
29	1.40			.091	4.00	.51
30	1.40			.14	4.00	.51
31	1.40			.20	4.00	.51
32	1.40			.20	4.00	.70
33	1.40	5	.02	.16	4.00	.79
34	1.40	5	.04	.20	2.00	.89
35	1.40	5	.04	.20	3.00	.89
36	1.40	5	.04	.20	4.00	.89
37	1.40	8	.04	.14	2.00	.56
38	1.40	8	.04	.14	3.00	.56
39	1.40	8	.04	.14	4.00	.56
40	1.40	5	.06	.26	4.00	1.02
41	1.90			.30	4.00	1.50
42	1.90			.45	4.00	1.50
43	1.90			.60	4.00	1.50
44	1.90			.45	4.00	1.00
45	1.90			.45	4.00	2.00
46	1.90			.45	3.00	1.50
47	1.90			.45	2.00	1.50
48	2.40			.70	4.00	2.50
49	2.40			.85	4.00	2.50
50	2.40			1.00	4.00	2.50
51	2.40			.85	4.00	2.00
52	2.40			.85	4.00	3.00
53	2.40			.85	3.00	2.50
54	2.40			.85	2.00	2.50